AD_____

Award Number: DAMD17-98-1-8171

TITLE: Epidermal Growth Factor Receptor Overexpression as a Target for Auger Electron Radiotherapy of Breast Cancer

PRINCIPAL INVESTIGATOR: Raymond M. Reilly, Ph.D.

CONTRACTING ORGANIZATION: The Toronto Hospital
Toronto, Ontario M5G 2C4 Canada

REPORT DATE: August 2002

TYPE OF REPORT: Final

PREPARED FOR: U.S. Army Medical Research and Materiel Command
Fort Detrick, Maryland 21702-5012

# REPORT DOCUMENTATION PAGE

*Form Approved*
*OMB No. 074-0188*



| 1. AGENCY USE ONLY (Leave blank) | 2. REPORT DATE | 3. REPORT TYPE AND DATES COVERED |
|---|---|---|
| | August 2002 | Final (1 Jul 98 - 1 Jul 02) |

**4. TITLE AND SUBTITLE**
Epidermal Growth Factor Receptor Overexpression as a Target for Auger Electron Radiotherapy of Breast Cancer

**5. FUNDING NUMBERS**
DAMD17-98-1-8171

**6. AUTHOR(S)**
Raymond M. Reilly, Ph.D.

**7. PERFORMING ORGANIZATION NAME(S) AND ADDRESS(ES)**
The Toronto Hospital
Toronto, Ontario M5G 2C4 Canada

E-Mail: raymond.reilly@utoronto.ca

**8. PERFORMING ORGANIZATION REPORT NUMBER**

**9. SPONSORING / MONITORING AGENCY NAME(S) AND ADDRESS(ES)**
U.S. Army Medical Research and Materiel Command
Fort Detrick, Maryland 21702-5012

**10. SPONSORING / MONITORING AGENCY REPORT NUMBER**



**11. SUPPLEMENTARY NOTES**
report contains color

**12a. DISTRIBUTION / AVAILABILITY STATEMENT**
Approved for Public Release; Distribution Unlimited

**12b. DISTRIBUTION CODE**

**13. Abstract** ***(Maximum 200 Words)*** *(abstract should contain no proprietary or confidential information)*
EGFR are overexpressed in the majority of ER-negative, hormone-resistant and poor prognosis breast cancers. Our goal is to exploit EGFR overexpression to selectively target the Auger electron-emitting radiopharmaceutical, $^{111}$In-hEGF to breast cancer cells for treatment of the disease. $^{111}$In-hEGF was highly radiotoxic *in vitro* to MDA-MB-468 breast cancer cells overexpressing EGFR (1-2 X $10^6$ receptors/cell) but not to MCF-7 breast cancer cells with a 100-fold lower level of EGFR. $^{111}$In-hEGF was >85-500 fold more cytotoxic to MDA-MB-468 cells than chemotherapeutic agents ($IC_{50}$ 70 pM vs. 6-30 nM) and low concentrations (70 pM) of $^{111}$In-hEGF produced the same growth inhibition as 4 Gy of γ-radiation. The radiopharmaceutical exhibited dose-related and strong selective anti-tumor effects against MDA-MB-468 tumors overexpressing EGFR implanted into mice. There were no changes in body weight, histopathological examination of liver and kidneys and serum ALT and Cr levels. There was a slight but not significant decrease in WBC and platelets. The radiopharmaceutical was most effective against small, non-established tumors. Our results are highly promising for the development of $^{111}$In-hEGF as a novel treatment for breast cancer.

| 14. SUBJECT TERMS | 15. NUMBER OF PAGES |
|---|---|
| breast cancer, auger electrons, indium-111, EGFR, EGF | 58 |
| | 16. PRICE CODE |

| 17. SECURITY CLASSIFICATION OF REPORT | 18. SECURITY CLASSIFICATION OF THIS PAGE | 19. SECURITY CLASSIFICATION OF ABSTRACT | 20. LIMITATION OF ABSTRACT |
|---|---|---|---|
| Unclassified | Unclassified | Unclassified | Unlimited |

## TABLE OF CONTENTS

**Preprint 1.** Wang J, Reilly RM, Chen P et al. Fusion of the $C_H1$ domain of $IgG_1$ to epidermal growth factor (EGF) prolongs its retention in the blood but does not increase tumor uptake. *Cancer Biother. and Radiopharm.* (in press) 2002.

**Reprint 2.** Wang J, Chen P, Su Z-F et al. Amplified delivery of indium-111 to EGFR-positive human breast cancer cells. *Nucl. Med. Biol.* 28: 895-902, 2001.

**Preprint 3**. Chen P, Mrkobrada M, Vallis KA et al. Comparative antiproliferative effects of $^{111}$In-DTPA-hEGF, chemotherapeutic agents and γ-radiation on EGFR-positive breast cancer cells. *Nucl. Med. Biol* . 2002 (in press)

## INTRODUCTION

The epidermal growth factor receptor (EGFR) is a transmembrane receptor tyrosine kinase which specifically binds human epidermal growth factor (hEGF) and is overexpressed in the majority (>90%) of estrogen receptor-negative, hormone-resistant and poor prognosis breast cancers (1). The level of EGFR overexpression in breast cancer may reach $10^6$ receptors/cell, more than 100-fold higher than on normal epithelial cells ($<10^4$ EGFR/cell). Binding of hEGF to the receptor activates an intracellular signaling pathway which ultimately results in upregulation of gene expression and cell division. hEGF is rapidly internalized into the cytoplasm following binding to its cell surface receptor, and a proportion of molecules are translocated to the cell nucleus (2). In this research project, it is hypothesized that the internalization and nuclear translocation of hEGF can be exploited to selectively insert the Auger electron-emitting radionuclide, indium-111 ($^{111}$In) into the cytoplasm and nucleus of breast cancer cells overexpressing EGFR, where the short-range electrons are highly damaging to DNA, resulting in cell death. The subcellular range of the Auger electrons should limit the radiotoxicity of the radiopharmaceutical to breast cancer cells which overexpress EGFR and are able to internalize sufficient quantities of the radionuclides. Since <3% of bone marrow stem cells express EGFR (3), the radiopharmaceutical in theory should not be toxic to the bone marrow, but may be toxic to normal tissues such as the liver and kidneys which express moderate levels of EGFR (~$10^5$ receptors/cell) (4,5). An objective of the research project is to evaluate the cytotoxicity of $^{111}$In-hEGF and a novel $^{111}$In-human serum albumin-hEGF bioconjugate ($^{111}$In-HSA-hEGF) against human breast cancer cells *in vitro* in comparison with conventional treatments for breast cancer such as chemotherapy and external γ-radiation. A second objective is to evaluate the anti-tumour effects and normal tissue toxicity of $^{111}$In-hEGF (or $^{111}$In-HSA-hEGF) against human breast cancer xenografts implanted in athymic mice *in vivo*. The rationale for using the $^{111}$In-HSA-hEGF bioconjugate was to increase the molecular size of hEGF to slow its blood clearance and promote tumour accumulation as well as provide sites for conjugation of multiple diethylenetriaminepentaacetic acid (DTPA) metal chelators for $^{111}$In to increase the specific activity of the radiopharmaceutical and thereby maximize the delivery of radioactivity to the tumours.

## BRIEF SUMMARY OF RESEARCH ACCOMPLISHED IN YEAR 1 (1998-1999)

The following represents a brief summary of the research accomplished in the 1st year of the project. Please consult the *August 1999 Annual Report* for a detailed description.

### *Task 1: Construction, expression, purification and testing of a novel hEGF-$C_H$1 fusion protein.*

In the 1st year of the project, a recombinant hEGF-$C_H$1 fusion protein was constructed, expressed in *E. coli* and tested for purity and receptor binding against MDA-MB-468 human breast cancer cells overexpressing EGFR [please see Reprint 1] (6) . The protein was successfully produced but only small quantities of correctly folded protein could be isolated and the protein was relatively insoluble which did not allow concentration which was required for DTPA derivatization and labeling with $^{111}$In. The research strategy was therefore changed to construct instead a human serum albumin (HSA)-hEGF bioconjugate which had properties similar to those

of the hEGF-$C_H1$ fusion protein (ie. higher molecular weight and multiple sites for DTPA derivatization) but was much more soluble. This task was completed.

**BRIEF SUMMARY OF RESEARCH ACCOMPLISHED IN YEAR 2 (1999-2000)**

The following represents a brief summary of the research accomplished in the 2nd year of the project. Please consult the *August 2000 Annual Report* for a detailed description.

***Task 2: Construction and purification of a novel human serum albumin (HSA)-hEGF bioconjugate***

A novel HSA-hEGF bioconjugate was constructed by chemically linking thiolated HSA with maleimide-derivatized hEGF [please see Reprint 2]. The HSA-hEGF bioconjugate was purified by ultrafiltration yielding a relatively homogeneous protein with $M_r$ 62-67 kDa by SDS-PAGE and size-exclusion HPLC which was positive for HSA and hEGF by Western blot. The bioconjugate was soluble in aqueous buffers and was easily concentrated to 5-10 mg/mL for derivatization with multiple DTPA metal chelators for labeling to high specific activity with $^{111}$In. This task was completed.

***Task 3: Radiolabeling of HSA-hEGF with $^{111}$In and testing for receptor binding, internalization and nuclear translocation in EGFR-overexpressing breast cancer cells***

HSA-hEGF retained its receptor-binding properties *in vitro* against MDA-MB-468 breast cancer cells, but the affinity constant ($K_a$) was reduced about 15-35 fold compared to hEGF. HSA-hEGF was derivatized with multiple DTPA metal chelators (as many as 23 per molecule) preferentially onto the HSA domain which significantly increased the specific activity when labeled with $^{111}$In compared to hEGF which could only be derivatized with a maximum of 1-2 DTPA metal chelators per molecule (7). Analogous to hEGF, HSA-hEGF was rapidly internalized into the cytoplasm and translocated to the cell nucleus in MDA-MB-468 breast cancer cells as assessed by fluorescence microscopy using fluorescein-derivatized bioconjugate and cell fractionation experiments using $^{111}$In-labeled bioconjugate. This task was completed.

***Task 4: In vitro testing of cytotoxicity of $^{111}$In-hEGF, chemotherapy and external γ-radiation against EGFR-overexpressing human breast cancer cells.***

The relative antiproliferative activity of $^{111}$In-hEGF against MDA-MB-468 breast cancer cells *in vitro* was compared with that of chemotherapeutic agents or external γ-radiation delivered by a $^{137}$Cs source [please see Reprint 3]. These experiments demonstrated that $^{111}$In-hEGF was at least 85-500 fold more cytotoxic (on a molar concentration basis) against EGFR-overexpressing breast cancer cells than the chemotherapeutic agents paclitaxel, doxorubicin, methotrexate or camptothecin and several logarithms more potent than 5-fluorouracil. The 50% cell growth inhibitory concentration ($IC_{50}$) was <70 pM for $^{111}$In-hEGF but was 6 nM for paclitaxel, 15-30 nM for doxorubicin, camptothecin and methotrexate and 4 μM for 5-fluorouracil. $^{111}$In-hEGF (70 pM) produced the same growth-inhibitory effect as 4 Gy of high dose rate external γ-radiation. This task was completed.

***Task 5: Comparison of the biodistribution and pharmacokinetics of $^{111}$In-HSA-hEGF and $^{111}$In-hEGF in mice implanted with human breast cancer xenografts.***

The biodistribution of $^{111}$In-HSA-hEGF was compared with that for $^{111}$In-hEGF in athymic mice implanted with subcutaneous MDA-MB-468 breast cancer xenografts. The tumour accumulation was not significantly increased for $^{111}$In-HSA-hEGF compared to $^{111}$In-hEGF (1.42 ± 0.37 % i.d./g vs. 1.17 ± 0.28 % i.d./g respectively) and tumour/blood ratios were lower (6.9 ± 1.9 vs. 10.3 ± 2.2 respectively) due to a prolonged retention of $^{111}$In-HSA-hEGF in the blood compared to $^{111}$In-hEGF (0.25 ± 0.02% i.d./g vs. 0.11 ± 0.02% i.d./g). Although the tumour accumulation of $^{111}$In-HSA-hEGF was not improved compared to $^{111}$In-hEGF, $^{111}$In-HSA-hEGF could deliver more radioactivity to the breast cancer cells *in vivo* due to a much higher specific activity when labeled with $^{111}$In, as a result of higher substitution with DTPA. This task was completed.

***Task 6: In vitro testing of $^{111}$In-HSA-hEGF bioconjugate for radiotoxicity against MDA-MB-468 and MCF-7 breast cancer cells.***

The antiproliferative effects of $^{111}$In-HSA-hEGF were evaluated *in vitro* against MDA-MB-468 breast cancer cells overexpressing EGFR (1-2 × $10^6$ receptors/cell). The specific activity of $^{111}$In-HSA-hEGF was increased 9-fold compared to $^{111}$In-hEGF due to multiple substitution of HSA-hEGF with DTPA metal chelators for $^{111}$In (7). The 9-fold higher specific activity yielded a 4-fold increased antiproliferative potency against MDA-MB-468 cells compared to $^{111}$In-hEGF ($IC_{50}$ 15 pM vs. 60 pM respectively). This task was completed.

**BRIEF SUMMARY OF RESEARCH ACCOMPLISHED IN YEAR 3 (2000-2001)**

The following represents a brief summary of the research accomplished in the 3rd year of the project. Please consult the *August 2001 Annual Report* for a detailed description.

***Task 4: Completion of studies examining the relative cytotoxicity of $^{111}$In-hEGF, chemotherapy and external γ-radiation against EGFR-positive breast cancer cells.***

Studies examining the cytotoxicity of $^{111}$In-hEGF *in vitro* against breast cancer cells were completed by determining the antiproliferative effects of the radiopharmaceutical in combination with chemotherapeutic agents or external γ-radiation (8). The results of these experiments [please see Reprint 3] demonstrated that the cytotoxic effects of chemotherapeutic agents or external γ-radiation were additive with those of $^{111}$In-hEGF. It was shown that low concentrations of chemotherapeutic agents in combination with $^{111}$In-hEGF increased the proportion of cell kill. Similar results were obtained with external γ-radiation. This task was completed.

***Task 6: Completion of studies examining the in vitro radiotoxicity of $^{111}$In-HSA-hEGF against MDA-MB-468 and MCF-7 breast cancer cells***

To complete the studies examining the cytotoxicity of $^{111}$In-HSA-hEGF against breast cancer cells, experiments were conducted to determine the selectivity of cytotoxicity of $^{111}$In-HSA-hEGF *in vitro* against MDA-MB-468 human breast cancer cells overexpressing EGFR (1-2 × $10^6$ receptors/cell) or MCF-7 breast cancer cells expressing a 100-fold lower level of EGFR on their

surface ($1 \times 10^4$ receptors/cell). These experiments demonstrated that $^{111}$In-HSA-hEGF was 4-fold more potent at inhibiting the growth of MDA-MB-468 cells than $^{111}$In-hEGF exhibiting an $IC_{50}$ of 15 pM vs. 60 pM respectively [please see Reprint 2]. $^{111}$In-HSA-hEGF and $^{111}$In-hEGF were also selectively cytotoxic to MDA-MB-468 breast cancer cells overexpressing EGFR but were not cytotoxic to MCF-7 breast cancer cells with a 100-fold lower level of EGFR expression. $^{111}$In-HSA-hEGF and $^{111}$In-hEGF were slightly growth stimulatory to MCF-7 cells, particularly at concentrations >100 pM. This is expected since breast cancer cells with low levels of EGFR are growth-stimulated by EGF whereas cells with high levels of EGFR are growth-inhibited (6). This task was completed.

***Task 7: Treatment of mice implanted with subcutaneous EGFR-positive MDA-MB-468 xenografts with $^{111}$In-HSA-hEGF or $^{111}$In-hEGF***

The anti-tumor effects and normal tissue toxicity of $^{111}$In-hEGF were evaluated *in vivo* in athymic mice implanted with subcutaneous MDA-MB-468 human breast cancer xenografts [please see Preprint 4]. Groups of 5 mice received five weekly s.c. injections of 500 μCi (17 μg) of $^{111}$In-hEGF (total 2.5 mCi). Control animals received injections of unlabeled hEGF (17 μg) or normal saline. $^{111}$In-hEGF completely arrested the growth of MDA-MB-468 tumors. Interestingly, treatment of mice with doxorubicin (5 mg/kg × 2 days) produced only a 2-fold tumor growth inhibition (not shown). Although tumors were only arrested by $^{111}$In-hEGF in this study, more recent experiments have shown that the anti-tumor effects of the radiopharmaceutical are tumor-size dependent and tumor regression can be achieved if $^{111}$In-hEGF treatment is started early when tumors are small (4 $mm^3$) rather than large (21 $mm^3$) (9). This effect is probably due to improved uptake and penetration of the radiopharmaceutical in small tumors. There was no significant change in body weight in mice treated with $^{111}$In-hEGF. Body weight was identical to that for control mice treated with unlabeled hEGF or normal saline, suggesting that there was no generalized normal tissue toxicity associated with the radiopharmaceutical. EM studies performed by Dr. Ross Cameron (a board-certified pathologist and co-investigator) of the liver and kidneys (the only normal tissues to express moderate levels of EGFR, ~$10^5$ receptors/cell) revealed no evidence of morphological damage. In contrast, mice treated with doxorubicin had a 20% decrease in body weight and 2/5 mice died of treatment-related toxicity. Extensive cardiotoxicity was also noted in mice treated with doxorubicin. No mice died of toxicity in the $^{111}$In-hEGF group. There was also no increase in ALT or SCr in mice treated with $^{111}$In-hEGF compared to control mice treated with saline confirming the absence of hepatotoxicity and renal toxicity. There was a modest decrease in WBC and platelets in mice treated with $^{111}$In-hEGF, but WBC values remained within the normal range and the decrease in platelet counts would not be clinically significant in humans. There was no decrease in RBC or hemoglobin with $^{111}$In-hEGF. The reason for decreased WBC and platelet counts is not known at present but may be due to non-specific irradiation of the bone marrow by the penetrating γ-emissions of $^{111}$In rather than specific radiotoxicity mediated by the short-range Auger electron emissions, since <3% of bone marrow stem cells are EGFR-positive (3) and capable of binding and internalizing $^{111}$In-hEGF. The $^{111}$In-HSA-hEGF bioconjugate was not tested *in vivo* for treatment of MDA-MB-468 breast cancer xenografts because it did not offer any advantages over $^{111}$In-hEGF in terms of tumor or normal tissue localization (see results from Task 5). This task was completed.

## SUMMARY OF RESEARCH ACCOMPLISHED IN YEAR 4 (2001-2002)

***Task 7: Completion of studies of treatment of mice implanted with subcutaneous EGFR-positive MDA-MB-468 or MCF-7 xenografts with $^{111}$In-hEGF***

In the final year of the project, additional more comprehensive studies examining the treatment of EGFR-overexpressing MDA-MB-468 human breast cancer xenografts with $^{111}$In-DTPA-hEGF or MCF-7 breast cancer xenografts with a 100-fold lower level of EGFR expression were conducted. This task was completed.

*Treatment of Established MDA-MB-468 Tumors*

Female, athymic mice were injected s.c. at multiple sites with $5 \times 10^6$ MDA-MB-468 breast cancer cells in 100 μL of culture medium. After 5-6 weeks, established s.c. tumors were visible with an average diameter (d) of approx. 3 mm corresponding to a tumor volume of 14-15 mm$^3$ assuming spherical geometry. Groups of 5-6 mice bearing a total of 15 tumors in each group were then treated with five weekly s.c. injections of 150 μCi (5.6 MBq; 1.0 μg), 300 μCi (11.1 MBq; 2.0 μg) or 500 μCi (18.5 MBq; 3.4 μg) of $^{111}$In-DTPA-hEGF or normal saline (control). The total amount of $^{111}$In-DTPA-hEGF administered was 750 μCi (27.8 MBq; 5.0 μg) to 2.5 mCi (92.5 MBq; 17 μg). The tumor diameter was measured every two-three days for 7 weeks using a precision caliper and the tumor volume calculated. A tumor growth index was calculated by dividing the tumor volume at each time point by the initial tumor volume. The mean tumor growth indices were plotted vs. the time since the start of treatment to obtain the tumor growth curves. The effect of treatment of athymic mice with five weekly amounts of 500 μCi (18.5 MBq; 0.7 μg) of $^{111}$In-DTPA-hEGF (total 2.5 mCi, 92.5 MBq; 3.4 μg) on the growth of established MDA-MB-468 breast cancer xenografts (initial tumor volume 14-15 mm$^3$) is shown in Fig. 1 A. Linear regression analysis of the tumor growth curves (not shown) revealed that the rate of tumor growth in mice treated with $^{111}$In-DTPA-hEGF was decreased 3-fold compared to that for control mice treated with normal saline (slope of tumor growth curve 0.0225 vs. 0.0737 day$^{-1}$; F-test, $p = 0.00204$). Tumor growth inhibition by $^{111}$In-DTPA-hEGF was dose-related. The tumor growth index at 20 days after commencing treatment for mice administered a total of 750 μCi (27.8 MBq), 1.5 mCi (55.5 MBq) or 2.5 mCi (92.5 MBq) of $^{111}$In-DTPA-hEGF was 4.45 ± 1.94, 2.88 ± 0.69 and 1.65 ± 0.21 respectively compared to 3.98 ± 1.14 for control animals treated with normal saline (Fig. 2 A). The tumor growth index at 49 days for mice treated with a total of 750 μCi (27.8 MBq), 1.5 mCi (55.5 MBq) or 2.5 mCi (92.5 MBq) of $^{111}$In-DTPA-hEGF was 3.37 ± 0.98, 2.58 ± 0.64 and 2.42 ± 0.62 respectively compared to 5.61 ± 1.67 for control mice treated with normal saline (Fig. 2 B).

*Treatment of Non-Established MDA-MB-468 Tumors*

The effect of early treatment with $^{111}$In-DTPA-hEGF on the growth of non-established MDA-MB-468 breast cancer xenografts was determined by implanting mice s.c. at multiple sites with $5 \times 10^6$ MDA-MB-468 cells. A total of 15-16 tumors (mean tumor volume 10 mm$^3$) were created in groups of 5 animals. In contrast to the previous study, radiopharmaceutical treatment was commenced only one week after tumor implantation. Mice received five weekly s.c. injections of $^{111}$In-DTPA-hEGF (500 μCi, 18.5 MBq; 3.4 μg each) or normal saline (control). The tumor diameter was measured every 2-3 days and the tumor volume and growth indices determined as previously described. The mean tumor growth index was plotted vs. the time since the start of

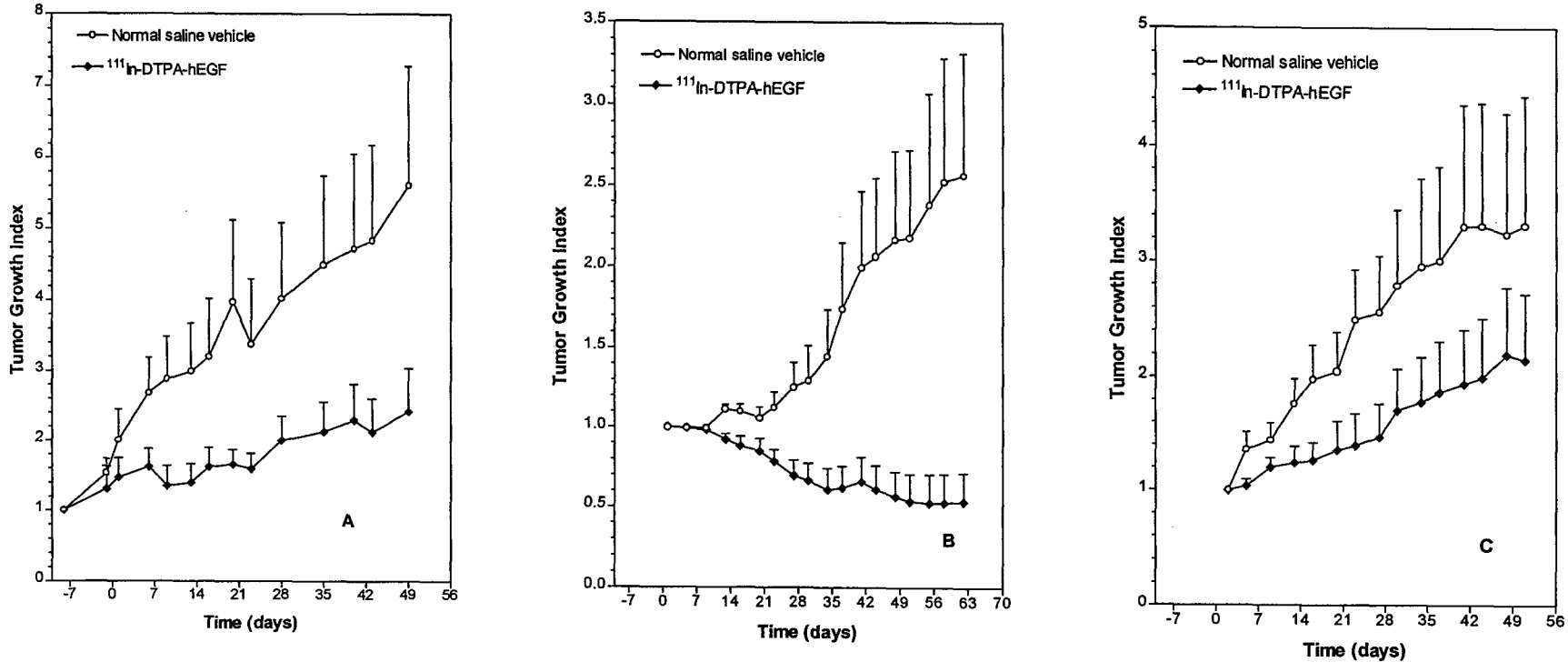


Fig. 1. A. Effect of treatment of established MDA-MB-468 human breast cancer xenografts in athymic mice with 92.5 MBq of $^{111}$In-DTPA-hEGF (17 μg) in five divided weekly doses. B. Effect of same treatment on non-established MDA-MB-468 xenografts. C. Effect of same treatment on MCF-7 breast cancer xenografts.

treatment to obtain the tumor growth curve. In contrast to established MDA-MB-468 tumors which were growth-inhibited by $^{111}$In-DTPA-hEGF (Fig. 1 A), non-established tumors (initial tumor volume 10 mm$^3$) exhibited tumor regression (Fig. 1 B) compared to normal saline treated control mice, which exhibited rapid tumor growth (slope –0.009 day$^{-1}$ vs. 0.0297 day$^{-1}$ respectively; F-test, $p < 0.0001$). The tumor growth index at 62 days was 0.53 ± 0.18 for $^{111}$In-DTPA-hEGF treatment vs. 2.57 ± 0.75 for normal saline treatment.

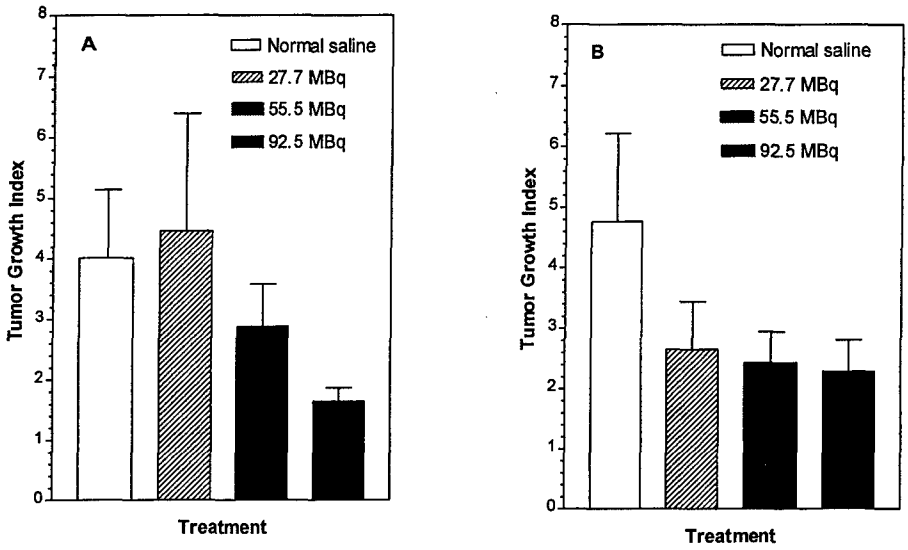


Fig. 2. Effect of treatment of established MDA-MB-468 human breast cancer xenografts with increasing amounts of $^{111}$In-DTPA-hEGF or normal saline at A. 20 days or B. 40 days after starting treatment. The total doses of the radiopharmaceutical investigated were 27.7 MBq (750 μCi), 55.5 MBq (1.5 mCi) and 92.5 MBq (2.5 mCi).

*Treatment of MCF-7 Tumors*

$^{111}$In-DTPA-hEGF also appeared to inhibit the growth of MCF-7 breast cancer xenografts (Fig. 1 C), but the difference in the slope of the tumor growth curve compared to that for normal saline treated control mice did not reach statistical significance (slope 0.0250 day-1 vs. 0.0488 day$^{-1}$ respectively; F-test, $p = 0.0509$). The tumor growth index at 51 days was 2.15 ± 0.57 for $^{111}$In-DTPA-hEGF treatment vs. 3.31 ± 1.11 for normal saline treated mice. These results suggested that the anti-tumor effects of the radiopharmaceutical were selective for EGFR-overexpressing breast cancer xenografts.

*Effect of Tumor Size on Radiopharmaceutical Uptake*

Since small, non-established MDA-MB-468 tumors responded better to $^{111}$In-DTPA-hEGF treatment, we conducted studies to examine the effect of tumor size on radiopharmaceutical accumulation. Ten female athymic mice were injected subcutaneously (s.c.) at multiple sites with $5 \times 10^5$ to $1 \times 10^7$ MDA-MB-468 human breast cancer cells in 100 μL of culture medium. After 4 weeks, tumors of different sizes (2-7 mm in diameter) were established (4-5 tumors/animal). The tumor volumes ranged from 5-200 mm$^3$ assuming a spherical geometry. The mice were then injected s.c. (at a site remote from tumor implantation) with 50 μCi (1.85 MBq; 0.3 μg) of $^{111}$In-

DTPA-hEGF. At 24 h post-injection (p.i.), the mice were sacrificed by cervical dislocation and tumors excised, weighed and counted along with a standard of the injected radiopharmaceutical in a γ-counter. For very small xenografts, multiple tumors were combined, weighed and the average weight and radioactivity concentration determined. The tumor uptake of $^{111}$In-DTPA-hEGF was expressed as percent injected dose/g (% i.d./g) and the relationship between radiopharmaceutical uptake and tumor size was examined. There was a strong inverse correlation between tumor uptake of $^{111}$In-DTPA-hEGF and tumor mass for very small tumors <5 mg (Fig. 3). The mean tumor uptake of $^{111}$In-DTPA-hEGF in tumors <5 mg (31.6 ± 7.5% i.d./g) was much greater than for 6-30 mg tumors (5.5 ± 0.5% i.d./g, $p < 0.001$) and some very small tumors (1-2 mg) showed exceptionally high accumulation of the radiopharmaceutical (>80 % i.d./g). There was also a small but significant decrease (not shown) in $^{111}$In-DTPA-hEGF uptake in tumors weighing 31-200 mg (3.4 ± 0.5% i.d./g, $p = 0.028$). Assuming a spherical geometry and a tissue density of 1 mg/mm$^3$, the range of tumor weights examined (<5mg, 6-30 mg and 31-200 mg) corresponded to tumors with diameter of <2 mm, 2-4 mm and 4-7 mm respectively and tumor volumes <5 mm$^3$, 6-30 mm$^3$ and 31-200 mm$^3$. The higher tumor accumulation of the radiopharmaceutical in small tumors likely explains the better response of small, non-established tumors to the radiopharmaceutical and suggests that the radiopharmaceutical may have a role in adjuvant treatment of breast cancer micrometastases.

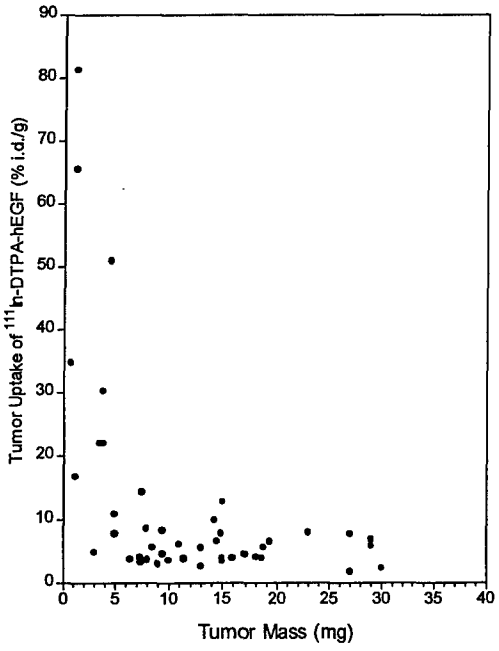


Fig. 3. Effect of tumor mass on accumulation of $^{111}$In-DTPA-hEGF in subcutaneous MDA-MB-468 human breast cancer xenografts implanted in athymic mice.

*Radation Microdosimetry Projections*

The radiation absorbed dose to the cell nucleus from $^{111}$In-DTPA-hEGF localized in individual MDA-MB-468 cells *in vivo* was projected based on a tumor uptake of 5 % i.d./g, 30 % i.d./g or 80 % i.d./g representing the wide range of radiopharmaceutical accumulation observed for tumors with volume 1-2 mm$^3$, 5 mm$^3$ or 6-30 mm$^3$ respectively (see *Effect of Tumor Size on Radiopharmaceutical Uptake* and Fig. 3). A total administered amount of 2.5 mCi (92.5 MBq) of $^{111}$In-DTPA-hEGF was assumed and the cumulative radioactivity in the tumor (Bq × sec) was

calculated by dividing the uptake in 1 g of tumor (Bq) by the decay constant for $^{111}$In ($3 \times 10^{-6}$ $sec^{-1}$) assuming rapid accumulation and no biological elimination of radioactivity from the tumor. The average cumulative radioactivity in each MDA-MB-468 cell (Ã, Bq × sec) was calculated assuming that 1 g of tumor with spherical geometry contains $2 \times 10^9$ cells based on a tissue density of 1 g/cm$^3$ and a cellular volume of $5 \times 10^{-10}$ cm$^3$ (diameter of $10^{-3}$ cm). The previously reported subcellular distribution for $^{111}$In-DTPA-hEGF in MDA-MB-468 cells *in vitro* (10) was used to proportion the cumulative amount of radioactivity ($\tilde{A}_S$, Bq × sec) to each source compartment (cell surface, cytoplasm and nucleus). The mean radiation absorbed dose to the cell nucleus (D, Gy) was estimated using the cellular dosimetry model of Goddu et al. (11) as $D = \tilde{A}_S \times S$, where S is the mean radiation absorbed dose to the nucleus per unit cumulated radioactivity in a source compartment (Gy/Bq.sec × $10^{-4}$). The radiation absorbed dose projections to the cell nucleus from $^{111}$In-DTPA-hEGF localized in MDA-MB-468 breast cancer xenografts at a tumor uptake level of 5, 30 or 80% i.d./g are shown in Table 1. It was assumed that the cellular distribution of $^{111}$In-DTPA-hEGF would be the same *in vivo* as that previously determined *in vitro* in MDA-MB-468 cells, ie. 20% remaining on the cell membrane, 65% present in the cytoplasm and 15% translocated to the cell nucleus (10). The S-factors for radiation deposited in the nucleus from radioactivity on the cell surface, in the cytoplasm or in the nucleus were $1.78 \times 10^{-2}$, $3.18 \times 10^{-2}$ and $60.30 \times 10^{-2}$ Gy/Bq.sec respectively (11). The radiation absorbed dose projections to the nucleus ranged from as low as 88 cGy (88 rads) at 5 % i.d./g to as high as 1,402 cGy (1,402 rads) at 80 % i.d./g (Table 1).

Table 1. Radiation absorbed dose projections for MDA-MB-468 human breast cancer cells in a s.c. tumor xenograft following treatment of mice with 92.5 MBq (2.5 mCi) of $^{111}$In-DTPA-hEGF in five divided weekly doses.

| | * Cumulative Radioactivity in Source Compartment ($\tilde{A}_S$, Bq × sec) | | |
|---|---|---|---|
| Tumor Uptake | 5 % i.d./g | 30 % i.d./g | 80 % i.d./g |
| Membrane | 154 | 924 | 2464 |
| Cytoplasm | 500 | 3,003 | 8,000 |
| Nucleus | 115 | 690 | 1,840 |
| Total | 769 | 4,617 | 12,304 |
| † Radiation Dose to Nucleus (D, cGy) | 88 | 529 | 1,402 |

Pharmacokinetic Studies

To characterize the disposition of $^{111}$In-DTPA-hEGF after subcutaneous (s.c.) injection (the route used for the treatment studies) versus intravenous (i.v) injection, detailed pharmacokinetic studies were performed. The pharmacokinetics of $^{111}$In-DTPA-hEGF after s.c. injection was studied in non-tumor bearing athymic mice. The mice were first anaesthetized by s.c. injection of ketamine/xylazine/acepromazine, then injected s.c. with 50 μCi (0.3 μg) of $^{111}$In-DTPA-hEGF. Blood samples were obtained at 5, 10, 20, and 30 mins and 1, 3, 6 and 24 h p.i. by knicking the tail of the mice with a sterile scalpel blade and collecting 22 μL of blood into heparinized microcapillary tubes. Blood samples were counted in a γ-counter and the concentration of $^{111}$In (cpm/μL) determined. The elimination phase of the blood radioactivity vs. time curve was fitted to a 2-compartment pharmacokinetic model using GraphPad Prism® software (12) and standard pharmacokinetic parameters ($t_{1/2}$, $V_d$, CL, MRT) were calculated. For comparison, in a separate

experiment, the blood and normal tissue concentrations of radioactivity 24 h after i.v. (tail vein), or s.c. injection of $^{111}$In-DTPA-hEGF (50 μCi, 1.85 MBq; 0.3 μg) to athymic mice were compared. $^{111}$In-DTPA-hEGF was rapidly absorbed within 20 mins following s.c. administration and quickly eliminated following biphasic kinetics (Fig. 4).

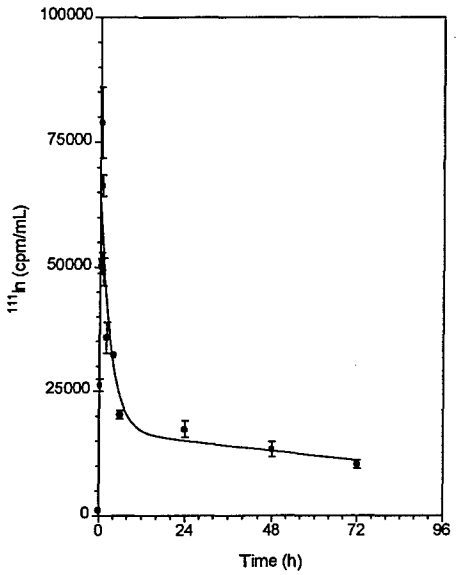


Fig. 4. Elimination of $^{111}$In-DTPA-hEGF from the blood after subcutaneous injection in non-tumor bearing athymic mice. The radiopharmaceutical exhibited a biphasic elimination pattern with an alpha phase half-life of 1.5 h and a beta phase half-life of 147 h.

The elimination phase was described by a 2-compartment pharmacokinetic model. The α-phase half-life was 1.5 h and the β-phase half-life was 146.7 h. The volume of distribution of the central compartment ($V_1$) was 13.2 mL (528 mL/kg for a 25 g mouse) and the volume of distribution at steady state ($V_{ss}$) was 34.2 mL (1,368 mL/kg). $V_1$ and $V_{ss}$ were about 7 times and 18 times greater respectively than the expected blood volume for a mouse (70-80 mL/kg) (13). The total body clearance ($CL_s$) of $^{111}$In-DTPA-hEGF was 0.16 mL/h (6.4 mL/kg × h). There were no significant differences in the concentration of radioactivity in the blood 24 h following s.c (0.17 ± 0.04 % i.d./g) or i.v. administration (0.27 ± 0.05 % i.d./g) of $^{111}$In-DTPA-hEGF ($p = 0.141$, Table 2). Similarly, there were no significant differences between the two routes of administration in liver or kidney uptake of $^{111}$In-DTPA-hEGF (Table 2).

Table 2. Comparison of the normal tissue accumulation of $^{111}$In-DTPA-hEGF 24 h after intravenous or subcutaneous administration in non-tumor bearing athymic mice.

| | * Normal Tissue Accumulation (percent injected dose/g) | |
|---|---|---|
| Tissue | Intravenous | Subcutaneous |
| Blood | †0.27 ± 0.05 | †0.17 ± 0.04 |
| Heart | 0.82 ± 0.15 | 0.51 ± 0.06 |
| Lungs | 1.23 ± 0.11 | 1.06 ± 0.24 |
| Liver | ‡18.30 ± 4.34 | ‡12.49 ± 4.08 |
| Stomach | 1.09 ± 0.09 | 1.15 ± 0.27 |
| Intestines | 2.96 ± 0.67 | 1.98 ± 0.29 |
| Spleen | 5.09 ± 1.01 | 2.44 ± 0.78 |
| Kidneys | ¶22.46 ± 4.01 | ¶18.26 ± 3.84 |

* Mean ± s.e.m. of 4-6 animals in each group.† Not significantly different (t-test, p = 0.141).
‡ Not significantly different (t-test, p = 0.362).¶ Not significantly different (t-test, p = 0.474).

***Task 8: Treatment of mice implanted with subcutaneous EGFR-positive MDA-MB-468 xenografts with $^{111}$In-hEGF in comparison with chemotherapy.***

Unfortunately, there was insufficient time remaining in the award period to conduct planned additional studies comparing the efficacy of treatment of MDA-MB-468 breast cancer xenografts with $^{111}$In-DTPA-hEGF or chemotherapeutic agents. Nevertheless, a detailed comparison of the antiproliferative effects of $^{111}$In-DTPA-hEGF in comparison to chemotherapeutic agents *in vitro* against MDA-MB-468 cells was conducted earlier in the project and reported previously (please see results from Task 4 and Preprint 3). In addition, a preliminary pilot study comparing $^{111}$In-DTPA-hEGF treatment and doxorubicin treatment of MDA-MB-468 xenografts was conducted and reported previously (please see results from Task 7). This task was also not in the original Statement of Work for the Award but was added to a revised Statement of Work in 2000. This task was partially completed.

***Task 9: Preparation and submission of manuscripts reporting the results of the research.***

During the award period (1998-2002), six full manuscripts were written describing the results of the research. Three of these manuscripts have been published in nuclear medicine or radiopharmaceutical peer-reviewed journals, two are in press and one is currently under preparation and will be submitted for publication within the next two months. In addition, six abstracts were presented at nuclear medicine or cancer research meetings and six presentations on targeted Auger electron radiotherapy were given by Dr. Reilly (P.I.) to nuclear medicine, medical physics or pharmacy audiences. A complete list of the manuscripts, abstracts and presentations is provided under *Reportable Outcomes.*

## KEY RESEARCH ACCOMPLISHMENTS

- Completed testing of the tumor growth-inhibitory properties of $^{111}$In-DTPA-hEGF against MDA-MB-468 breast cancer xenografts overexpressing EGFR or MCF-7 breast cancer xenografts expressing a 100-fold lower level of EGFR in athymic mice. Tested increasing doses of the radiopharmaceutical and its effectiveness against established or non-established MDA-MB-468 tumors. These studies clearly showed that $^{111}$In-DTPA-hEGF exhibited potent and selective anti-tumor effects against MDA-MB-468 xenografts overexpressing EGFR which were dose-related, were most effective against small, non-established tumors and were associated with minimal normal tissue toxicity.

- Determined the effect of tumor size on $^{111}$In-DTPA-hEGF tumor accumulation. These studies showed that a much higher uptake of the radiopharmaceutical was achieved in smaller MDA-MB-468 tumors compared to larger tumors. These results provide a possible hypothesis for the greater antiproliferative effects of the radiopharmaceutical against small, non-established tumors.

- Performed microdosimetry calculations to estimate the radiation absorbed dose to MDA-MB-468 cells in a tumor nodule from administration of the radiopharmaceutical depending on the level of tumor accumulation.

- Conducted detailed studies to determine the pharmacokinetics of $^{111}$In-DTPA-hEGF following intravenous or subcutaneous administration to athymic mice. These studies showed that the radiopharmaceutical was rapidly absorbed and eliminated from the blood following subcutanous administration. There were no significant differences between intravenous or subcutaneous administration routes in normal tissue accumulation.

## REPORTABLE OUTCOMES

### Manuscripts

1. Chen P, Cameron R, Wang J, Vallis KA, Sandhu J, Hendler A and Reilly RM. $^{111}$In-labeled epidermal growth factor has potent growth-inhibitory effects on human breast cancer xenografts in athymic mice. (in preparation) 2002. [Senior responsible author].

2. Wang J, Reilly RM, Chen P, Yang S, Bray MR, Gariepy J, Chan C and Sandhu J. Fusion of the $C_H1$ domain of $IgG_1$ to epidermal growth factor (EGF) prolongs its retention in the blood but does not increase tumor uptake. *Cancer Biother. Radiopharm.* (in press) 2002. [Senior responsible author].

3. Chen P, Mrkobrada M, Vallis K, Sandhu J, Cameron R, Hendler A and Reilly RM. Comparative antiproliferative effects of $^{111}$In-DTPA-hEGF, chemotherapeutic agents and $\gamma$-radiation on EGFR-positive breast cancer cells. *Nucl. Med. Biol.* (in press), 2002. [Senior responsible author].

4. Wang J, Chen P, Su ZF, Vallis K, Sandhu J, Hendler A, Cameron R and Reilly RM. Amplified delivery of indium-111 to EGFR-positive breast cancer cells. *Nucl. Med. Biol.* 28: 895-902, 2001. [Senior responsible author].

5. Reilly RM, Kiarash R, Sandhu J, Lee YW, Cameron R, Hendler A, Vallis K and Gariépy J. A comparison of epidermal growth factor and monoclonal antibody 528 labeled with indium-111 for imaging human breast cancer. *J. Nucl. Med.* 41: 903-911, 2000. [Principal author].

6. Reilly RM, Kiarash R, Cameron R, Porlier N, Sandhu, J, Vallis K, Hendler A, Hill RP and Gariépy J. Indium-111 EGF is selectively radiotoxic to human breast cancer cells overexpressing EGFR. *J. Nucl. Med.* 41: 429-438, 2000. [Principal author].

### Abstracts

1. Reilly RM, Chen P, Wang J, Vallis KA, Cameron R and Hendler A. Novel targeted Auger electron radiotherapy strongly inhibits the growth of human breast cancer xenografts in mice with minimal normal tissue toxicity. Accepted for presentation at Era of Hope Department of

Defense Breast Cancer Research Program Meeting, Orlando, FL, September 25-28, 2002. [Senior responsible author].

2. Chen, P., Cameron, J., Wang, J., Vallis, K., Sandhu, J., Hendler, A.L. and Reilly, R..M. The anti-tumor effect of the Auger electron-emitting radiopharmaceutical, $^{111}$In-hEGF against MDA-MB-468 human breast cancer xenografts is tumor-size dependent. *J. Nucl. Med.* 45: 255P [Abstract 1073]. [Senior responsible author].

3. Chen, P., Brandwein, J. Wedel, N., O'Connor, J. and Reilly, R.M. $^{111}$In-labeled humanized monoclonal antibody HuM195 is selectively radiotoxic to human leukemia cells expressing CD33. *J. Nucl. Med.* 45: 255P [Abstract 1072]. [Senior responsible author].

4. Chen, P., Mrkobrada, M., Vallis, K. and Reilly, R.M. Comparison of the cytotoxic effects of targeted Auger electron radiotherapy, external γ-radiation and cancer chemotherapeutics against EGFR-positive human breast cancer cells. *Proc. American Assoc. Cancer Research* 91st Annual Meeting 2000. [abstract] [Senior responsible author].

5. Wang J., Sandhu, J., Chen Z., Leung C., Bray M., Yang M., Cameron R., Hendler A., Vallis K., Reilly R.M. Production of a human epidermal growth factor (hEGF)-immunoglobulin ($C_H1$) fusion protein for targeting human breast cancer. *Clin. Cancer Res.* 1999 [abstract] [Senior responsible author].

6. Wang J., Sandhu, J., Chen Z., Leung C., Bray M., Yang M., Cameron R., Hendler A., Vallis K., Reilly R.M. Production of a human epidermal growth factor (hEGF)-immunoglobulin ($C_H1$) fusion protein for targeting human breast cancer. *J. Nucl. Med.* 1999 [abstract] [Senior responsible author].

**Presentations**

1. Reilly, R.M. Auger electron-emitting radiopharmaceuticals as novel therapeutic agents for cancer. Presented at Pharmaceutical Sciences graduate seminar, January 18, 2002. [Principal author]

2. Reilly, R.M. Targeted Auger electron radiotherapy of breast cancer and other malignancies. Presented at the meeting of the Toronto Nuclear Medicine Society, November 15, 2001. [Principal author]

3. Reilly, R.M. Molecular imaging and targeted radiotherapy of cancer: Past, present and future. Presented at Department of Medical Biophysics seminar, Sunnybrook and Women's College Health Sciences Centre, Toronto, ON, July 4, 2001. [Principal author]

4. Reilly, RM. Targeted Auger electron radiotherapy of malignancies. Presented at the Ontario Association of Medical and Radiological Technologists meeting, Richmond Hill, May 5, 2001. [Principal author].

5. Reilly, RM. Targeted Auger electron radiotherapy of malignancies. Presented at Nuclear Medicine Rounds, University Hospital, London, ON, April 19, 2000 [Principal author]

6. Reilly RM. The Trojan Horse: Targeted auger electron radiotherapy of breast cancer. Presented at Department of Radiation Oncology Rounds, University of Toronto, February 25, 1999 [Principal author]

**Media Coverage**

1. National Post Newspaper, Toronto, June 25, 2001. *Scientists Test New Cancer Weapon.* Heather Sokoloff. Story about preclinical testing of a new radiopharmaceutical treatment for advanced breast cancer.

**Applications for Funding Based on Research**

*U.S. Army Breast Cancer Research Program.* 2002-2004. R.M. Reilly (P.I.), K. A. Vallis, A. Oza, G. Lockwood, A. Hendler, R. Cameron. Preclinical lead-up studies in support of an IND application for $^{111}$In-hEGF, A new radiopharmaceutical for treatment of advanced breast cancer. $ 199,595 U.S. awarded.

*Susan G. Komen Breast Cancer Foundation.* 2001-2003. K. A. Vallis (P.I.), R.M. Reilly (Co.I.), A. Oza, G. Lockwood, A. Hendler, R. Cameron, W. Wells and D. Warr. A Phase I Study of $^{111}$In-Epidermal Growth Factor. A Novel Radiopharmaceutical Agent for the Treatment of Breast Cancer. $ 250,000 U.S. awarded.

*Canadian Institutes of Health Research (CIHR).* 2002-2005. R.M. Reilly (P.I.), J. Brandwein, J. Dick and M. Minden. Novel targeted Auger electron radiotherapy of acute myelogenous leukemia. $ 210,000 awarded.

*James Birrell Neuroblastoma Research Fund.* 2001-2002. R.M. Reilly (P.I.) and S. Baruchel (Co.I.). Novel targeted Auger electron radiotherapy of neuroblastoma using $^{123}$I-MIBG. $ 25,000 awarded.

*Natural Sciences and Engineering Research Council of Canada* 2000-2003. Vascular growth factor receptors as a target for Auger electron radiotherapy of malignant astrocytomas. J. Sandhu, R.M. Reilly (Co.I.) and A. Guha. $ 252,000 awarded.

**CONCLUSIONS AND FUTURE RESEARCH**

We conclude that $^{111}$In-hEGF is a highly promising new targeted adiotherapeutic agent for advanced, estrogen receptor-negative and EGFR-positive, hormone-resistant breast cancer. The radiopharmaceutical is highly and selectively cytotoxic *in vitro* to human breast cancer cells overexpressing EGFR. $^{111}$In-hEGF exhibits strong antiproliferative effects on breast cancer cells *in vitro* at concentrations at least 85-500 fold lower than those required for commonly used chemotherapeutic drugs. Treatment of mice implanted subcutaneously with human breast cancer xenografts overexpressing EGFR with 5 × 500 μCi (18.5 MBq) doses of $^{111}$In-hEGF strongly

inhibited the growth of the tumours in comparison to control mice treated with unlabeled hEGF or normal saline and tumor regression could be achieved if treatment was started within one week after implantation of breast cancer cells. There was no significant change in body weight following treatment with $^{111}$In-hEGF indicating no generalized normal tissue toxicity. There was also no evidence of damage to the liver or kidneys by electron microscopy or by measuring serum ALT and creatinine. There was a slight, but not clinically significant decrease in peripheral blood leukocytes and platelets. Based on these highly promising preclinical results with $^{111}$In-hEGF against breast cancer cell lines and tumour xenografts implanted in mice supported by the *IDEA Award*, we are now planning a Phase I clinical trial of the radiopharmaceutical in breast cancer patients, which we hope to commence at the University Health Network by 2003. An application was submitted in 2002 to the U.S. Army Breast Cancer Research Program for a *Clinical Bridge Award* to support the development of a clinical quality formulation and to collect supporting data for an Investigational New Drug (IND) application to Health Canada for $^{111}$In-hEGF. Support was also requested in the form of a *Clinical-Translational Research Award* for the Phase I clinical trial from the Susan G. Komen Breast Cancer Foundation. Both the U.S. Army Clinical Bridge Award and the *Clinical-Translational Research Award* from the Susan G. Komen Breast Cancer Foundation were awarded.

## REFERENCES


1. Klijn JGM, Berns PMJ, Schmitz PIM, Foekens JA. The clinical significance of epidermal growth factor receptor (EGF-R) in human breast cancer: a review on 5232 patients. *Endocr. Rev.* 1992; 13: 3-17.

2. Rakowicz-Szulcynska EM, Rodeck U, Herlyn M, Koprowski H. Chromatin binding of epidermal growth factor, nerve growth factor, and platelet-derived growth factor in cells bearing the appropriate surface receptors. *Proc. Natl. Acad. Sci.* USA 1986; 83: 3728-3732.

3. Waltz TM, Malm C, Nishikawa BK, Wasteson A. Transforming growth factor-alpha (TGF-alpha) in human bone marrow: demonstration of TGF-alpha in erythroblasts and eosinophilic precursor cells and of epidermal growth factor receptors in blastlike cells of myelomonocytic origin. *Blood* 1995; 85: 2385-2392.

4. Dunn WA, Hubbard AL. Receptor-mediated endocytosis of epidermal growth factor by hepatocytes in the perfused rat liver: ligand and receptor dynamics. *J. Cell Biol.* 1984; 98: 2148-2159.

5. Fisher DA, Salido EC, Barajas L. Epidermal growth factor and the kidney. *Ann. Rev. Physiol.* 1989; 51: 67-80.

6. Filmus J, Pollak MN, Cailleau R, Buick RN. A human breast cancer cell line with a high number of epidermal growth factor (EGF) receptors, has an amplified EGF receptor gene and is growth inhibited by EGF. *Biochem Biophys Res Commun* 1985; 128: 898-905.

7. Wang J, Chen P, Su Z-F, Vallis K, Sandhu J, Cameron R, Hendler A and Reilly RM. Amplified delivery of indium-111 to EGFR-positive breast cancer cells. *Nucl. Med. Biol.* 2001 (submitted).

8. Chen P, Mrkobrada M, Vallis KA, Sandhu J, Cameron R, Hendler A and Reilly RM. Comparative antiproliferative effects of novel targted Auger electron radiotherapy, chemotherapy and external γ-radiation on EGFR-overexpressing breast cancer cells. *Int J. Cancer* 2001 (submitted).

9. Chen, P., Cameron, J., Wang, J., Vallis, K., Sandhu, J., Hendler, A.L. and Reilly, R..M. The anti-tumor effect of the Auger electron-emitting radiopharmaceutical, $^{111}$In-hEGF against MDA-MB-468 human breast cancer xenografts is tumor-size dependent. *J. Nucl. Med.* 45: 255P [Abstract 1073].

10. Reilly RM, Kiarash R, Cameron R, Porlier N, Sandhu, J, Vallis K, Hendler A, Hill RP and Gariépy J. Indium-111 EGF is selectively radiotoxic to human breast cancer cells overexpressing EGFR. *J. Nucl. Med.* 41: 429-438, 2000.

11. Goddu S, Howell RW and Rao DV. Cellular dosimetry: absorbed fractions for monoenergetic electron and alpha particle sources and S-values for radionuclides uniformly distributed in different cell compartments. *J. Nucl. Med.* 35: 303-316, 1994.

12. Motulsky HJ, Stannard P, Neubig R, Prism. Ver 2.0. San Diego, GraphPad Software Inc. 1995

13. Olfert ED, Cross BM, McWilliam AA. Guide to the Care and Use of Experimental Animals. Vol. 1, Canadian Council on Animal Care (CCAC), Ottawa, 1993.

# APPENDICES

Short Communication

# Fusion of the $C_H1$ Domain of $IgG_1$ to Epidermal Growth Factor (EGF) Prolongs its Retention in the Blood but Does Not Increase Tumor Uptake

**Judy Wang [1], Raymond M. Reilly [1, 5, 6], Paul Chen [1], Shaoxian Yang [2], Mark R. Bray [3], Jean Gariépy [2, 7], Conrad Chan [4] and Jasbir Sandhu [4]**

[1]Division of Nuclear Medicine, University Health Network, [2]Ontario Cancer Institute, Princess Margaret Hospital, [3]Amgen Research Institute, [4]Samuel Lunenfeld Research Institute, Mount Sinai Hospital, [5]Departments of Medical Imaging, [6]Pharmaceutical Sciences, and [7]Medical Biophysics, University of Toronto, Toronto, ON, Canada M5G 2C4

Address reprint requests to Dr. Raymond M. Reilly, Division of Nuclear Medicine, Toronto General Hospital, University Health Network, 200 Elizabeth Street, Toronto, ON, Canada, M5G 2C4. Phone: 416-340-3036; Fax: 416-340-5065; E-mail: raymond.reilly@utoronto.ca

## ABSTRACT

An expression vector (pJW4) for a human epidermal growth factor (hEGF)-$C_H1$ fusion protein was constructed by fusing the gene for hEGF with the gene for $C_H1$ of murine $IgG_1$ with/without a peptide linker sequence [$(GGGGS)_3$] and inserting the recombinant gene into vector pGEX2T. Expression vector pGEX2T was transfected into E. coli (BL-21) and hEGF-$C_H1$ expressed by induction of the lac $I^q$ promotor with 50 μM isopropyl β-D-thiogalactopyranoside (IPTG). hEGF-$C_H1$ fused to glutathione S-transferase (GST) was isolated and purified by affinity chromatography. GST was cleaved using thrombin. SDS-PAGE demonstrated a protein with the expected $M_r$ (18 kDa) positive for hEGF by Western blot. hEGF-linker-$C_H1$ exhibited preserved binding to A431 (2-3 × $10^6$ EGFR/cell) and MDA-MB-468 breast cancer cells (1-2 × $10^6$ EGFR/cell). hEGF-$C_H1$ without the linker exhibited poor receptor binding. hEGF-linker-$C_H1$ also exhibited strong binding to soluble EGFR equivalent to that of hEGF. The tumor and normal tissue distribution of hEGF-linker-$C_H1$ labeled with $^{123}I$ was compared with $^{123}I$-hEGF at 24 h after i.v. injection to mice implanted with s.c. MDA-MB-468 xenografts. Fusion of hEGF with $C_H1$ increased its retention in the blood 14-fold but did not significantly increase tumor uptake. Tumor/blood ratios were higher for hEGF than for hEGF-linker-$C_H1$. We conclude that hEGF is more attractive than hEGF-linker-$C_H1$ for imaging EGFR-positive tumors.

**Key words**: epidermal growth factor, immunoglobulin, fusion protein, iodine-123

## INTRODUCTION

Overexpression of epidermal growth factor receptors (EGFR) is a property of estrogen receptor-negative, hormone-resistant and poor prognosis breast cancers [1]. We previously demonstrated that EGFR-positive MDA-MB-468 human breast cancer xenografts implanted subcutaneously (s.c.) in athymic mice could be imaged using hEGF labeled with $^{111}$In [2]. Tumor uptake of hEGF was relatively low however (1-2 % injected dose/g), possibly due to the rapid renal elimination of the peptide from the blood [2]. One strategy which has been shown to slow the blood clearance of scFv antibody fragments and promote their tumor accumulation is to fuse the fragments with an immunoglobulin sequence (eg. $C_H3$ domain, "minibodies") [3]. In this communication, we describe the synthesis of a novel recombinant hEGF immunoglobulin fusion protein with/without a flexible polypeptide linker sequence [$(GGGGS)_3$] inserted between hEGF and the $C_H1$ domain of murine $IgG_1$. The $C_H1$ domain was selected to minimize dimerization of the hEGF-immunoglobulin fusion protein which occurs with scFv-$C_H3$ "minibodies" [3] due to the strong interaction between $C_H3$ domains. Although dimerization would increase the size of the fusion protein and may potentially slow its renal elimination, there is a concern that it may diminish tumor penetration. Murine $C_H1$ was selected for this "proof-of-principle" study due to the commercial availability of the vector containing this sequence, but in future studies human $C_H1$ would be desireable to minimize immunogenicity. The hEGF-linker-$C_H1$ fusion protein was radiolabeled with $^{123}$I and its blood clearance and tumor and normal tissue accumulation evaluated in athymic mice bearing s.c. MDA-MB-468 human breast cancer xenografts compared to $^{123}$I-hEGF.

## MATERIALS AND METHODS

### Construction of Plasmids Expressing hEGF-$C_H1$

The hEGF gene was amplified from plasmid pADH59 (ATCC, Manassis, VA) by PCR using forward (5'-GAAGTTAAACTGCAGAACTCTGATTCCGAATGCCC-3') and reverse hEGF (5'-TGAGGAGACGGTGACCGTACGCAGTTCCCACC-3') or reverse hEGF-linker (5'-GACGGTGACCGTAGATCCGCCGCCACCCGACCCACCACCGCCCGAGCCACCGCCACCACG CAGTTCCC-3') primers containing *Pst I* and *Bst EII* restriction sites (underlined) respectively. The amplified hEGF gene was cut with *Pst I* and *Bst EII* (MBI Fermentas, Flamborough, ON), purified on a 2% agarose gel and ligated at the *Pst I* and *Bst EII* restriction sites into plasmid pASK84 (ATCC) [4] containing the $C_k$ and $C_H1$ gene of murine $IgG_1$. The hEGF-$C_H1$ or hEGF-linker-$C_H1$ gene was amplified from pASK84 by PCR using hEGF-$C_H1$ forward (5'-GTTAAAGGATCCAACTCTGATTCCGAATGCCC-3') and reverse (5'-GTAGTCGAA TTCATGGTGATGGTGGTGATG-3') primers containing the *Bam HI* and *Eco RI* restriction sites (underlined) respectively. The PCR conditions were: 5% DMSO, 2.5 mM $MgCl_2$, 0.25 mM of each dNTP, 0.5 μM of primers and 2.5 units of Pwo DNA polymerase (Boehringer-Mannheim, Laval, PQ). The PCR protocol was: 1 min at 94 °C (prior to adding Pwo DNA polymerase) followed by 30 cycles of 30 secs each at 94 °C, 58 °C for 30 secs and 72 °C for 1 min. PCR products were electrophoresed on a 2% agarose gel and purified using the QIAEX PCR purification kit (Qiagen, Mississauga, ON). PCR products were cut with *Bam HI* and *Eco RI*, purified on a 2% agarose gel and ligated into plasmid pGEX2T (Amersham-Pharmacia Biotech, Baie d'Urfé, PQ) at the *Bam HI* and *Eco RI* restriction sites to produce the final expression vector, pJW4. pJW4 expressed hEGF-$C_H1$ or hEGF-linker-$C_H1$ fused to a glutathione S-transferase (GST) affinity tag under control of the lac $I^q$ promotor induced by isopropyl β-D-thiogalactopyranoside (IPTG). The sequence and correct reading frame of the hEGF-$C_H1$ or

hEGF-linker-$C_H1$ inserts were confirmed by DNA sequencing (Core Molecular Biology Laboratory, York University, Toronto, ON).

**Expression and Purification of hEGF-$C_H1$ and hEGF-Linker-$C_H1$**

The pJW4 vector containing the hEGF-$C_H1$ gene was transfected into E. coli (BL-21) using the heat shock method [5]. Cultures were grown at 37 °C in LB broth containing 100 μg/mL of ampicillin to an absorbance of 0.6-0.8 measured at 600 nm. Expression of the hEGF-$C_H1$ or hEGF-linker-$C_H1$ proteins was induced by 50 μM IPTG (Sigma, St. Louis, MO) for 2 h. hEGF-$C_H1$ or hEGF-linker-$C_H1$ was isolated under native conditions from a 1 L culture by centrifugation for 1 min at 15,000 × g and lysing the bacterial pellet (1-2 mL) in 50 mM Tris-HCl buffer pH 8.0 containing 1 mM disodium EDTA and 100 μg/mL of lysozyme (Sigma) on ice for 15 mins. Dithiothreitol (DTT, Sigma) and sarkosyl (Sigma) were added to the lysate to a final concentration of 5 mM and 1.5% respectively. The lysate was centrifuged at 15,000 × g for 10 min and the supernatant containing hEGF-$C_H1$ or hEGF-linker-$C_H1$ purified using glutathione-Sepharose 4B resin (Amersham-Pharmacia Biotech, Inc.). Purified hEGF-$C_H1$ and hEGF-linker-$C_H1$ were recovered in a concentration of 75-100 μg/mL and the GST affinity tag was cleaved using thrombin (10 units/mg protein) at room temperature overnight.

**SDS-PAGE and Western Blot Analysis**

SDS-PAGE was performed on the hEGF-linker-$C_H1$ fusion protein using a 4-20% Tris-HCl gradient gel (BioRad, Mississauga, ON) under reducing conditions stained with Coomassie R-250 blue (BioRad) and by Western blot using a polyclonal anti-hEGF rabbit antibody (supplied by Dr. J. Gariépy, Ontario Cancer Institute). Reactive bands on Western blot were detected using a goat anti-rabbit antibody-horseradish peroxidase conjugate followed by diamidobenzidine (DAB, Sigma) chromogenic substrate and 0.03% $H_2O_2$.

**Evaluation of Receptor-Binding Properties by Flow Cytometry and ELISA**

The receptor-binding properties of hEGF-$C_H1$ with/without the polypeptide linker sequence were evaluated in comparison to hEGF by incubation of the proteins (5 μg/mL in PBS) with $3 \times 10^5$ A431 ($2\text{-}3 \times 10^6$ EGFR/cell) [6] or MDA-MB-468 cells ($1\text{-}2 \times 10^6$ EGFR/cell) [7] for 45 mins at 4 °C. The cells were washed with PBS and incubated with FITC-labeled anti-hEGF antibody for 45 mins at 4 °C. The cells were washed again and analyzed in an Epics XL-MCL flow cytometer (Beckman-Coulter, Palo Alto, CA). ELISA was performed to compare the receptor binding of hEGF and hEGF-linker-$C_H1$. A microtiter plate (EIA/RIA polystyrene plate, Costar) was coated overnight at 4 °C with soluble EGFR isolated from MDA-MB-468 cells as described by Gregoriou [8]. The wells were pre-treated with 5% skimmed milk for 2 h at 37 °C to block non-specific binding sites and then increasing concentrations of hEGF or hEGF-linker-$C_H1$ (10, 70 or 200 nM) were incubated in the wells for 45 mins at 37 °C. The wells were washed five times with PBS containing 0.05% Tween-20 to remove unbound EGF or EGF-linker-$C_H1$. Detection of receptor-bound EGF or EGF-linker-$C_H1$ was achieved by incubating first with rabbit anti-EGF polyclonal antibody (1:1000 dilution in PBS/0.05% Tween-20) for 45 mins at 37 °C, washing five times with PBS/0.05% Tween-20 and then incubating with goat anti-rabbit-horseradish peroxidase conjugate (1:2000 dilution in PBS/0.05% Tween-20, Sigma) for 45 mins at 37 °C. The chromogenic reagent, TMBZ (tetramethylbenzidine dihydrochloride, Sigma) and 0.03% $H_2O_2$ was

then added. The reaction was stopped after 5 mins with 1 N $H_2SO_4$ and the color measured at 450 nm in a plate reader.

### Tumor and Normal Tissue Biodistribution of hEGF-Linker-$C_H1$ and hEGF Labeled with $^{123}I$

Purified hEGF-linker-$C_H1$ and hEGF (Upstate Biotechnology, Lake Placid, NY) were labeled with $^{123}I$ (MDS-Nordion, Kanata, ON) using the chloramine-T method as previously described [2] . $^{123}I$-hEGF-linker-$C_H1$ or $^{123}I$-hEGF were purified from free $^{123}I$ on a Sephadex G-25 (Amersham-Pharmacia Biotech) or P-2 (BioRad) mini-column respectively eluted with 150 mM sodium chloride. The radiochemical purity of $^{123}I$-hEGF-linker-$C_H1$ and $^{123}I$-hEGF was >98% assessed by paper chromatography developed in 85% methanol. The tumor and normal tissue distribution of the radiopharmaceuticals were evaluated in athymic mice implanted s.c. with MDA-MB-468 human breast xenografts. Mice were injected i.v. (tail vein) with 5 μCi (0.5 μg) of $^{123}I$-hEGF-linker-$C_H1$ or $^{123}I$-hEGF and sacrificed at 24 hours post-injection by cervical dislocation. The tumor and samples of blood and normal tissues were obtained, weighed and counted along with a sample of the injected radiopharmaceutical in a gamma counter. Tumor and normal tissue uptake were expressed as percent injected dose/g (% i.d./g) and tumor/normal tissue (T/NT) ratios. Statistical comparisons were made using Student's t-test ($p<0.05$). Animal studies were conducted under an approved protocol from the Animal Care Committee at the University Health Network (No. 94-036).

## RESULTS AND DISCUSSION

### Construction of plasmids

DNA sequencing confirmed that the pJW4 expression vector contained the complete DNA sequence in the correct reading frame for the hEGF-$C_H1$ or hEGF-linker-$C_H1$ fusion proteins. The pJW4 plasmid expressed hEGF-$C_H1$ or hEGF-linker-$C_H1$ fused to GST and a 6-mer polyhistidine affinity tag at the C-terminus of the $C_H1$ domain. The polyhistidine tag was co-amplified with the $C_H1$ domain sequence from pADH59 and provided an alternative means of purification by metal affinity chromatography, not exploited in the current work. In this study, GST was used as the affinity tag for purification and the GST fusion partner was ultimately cleaved using thrombin.

### Expression and Purification of hEGF-$C_H1$ and hEGF-linker-$C_H1$

The hEGF-$C_H1$ or hEGF-linker-$C_H1$ fusion proteins were expressed in E. coli (BL-21). The overall yield of hEGF-$C_H1$ or hEGF-linker-$C_H1$ was approx. 1-2 mg/L but most of the fusion proteins were contained in inclusion bodies. Attempts at refolding hEGF-$C_H1$ or hEGF-linker-$C_H1$ by rapid dilution with reduction by dithiothreitol (DTT) [9] did not yield a useful protein, but smaller amounts (100-200 μg/L) of soluble, properly-folded hEGF-$C_H1$ or hEGF-linker-$C_H1$ proteins were isolated from the cytoplasm of E. coli under native conditions, and successfully purified by affinity chromatography using glutathione-Sepharose 4B resin. The insolubility of hEGF-$C_H1$ or hEGF-linker-$C_H1$ may be due to misfolding of the hEGF moiety due to incorrectly formed disulfide bonds. hEGF contains 3 disulfide bonds which are essential to maintain its tertiary structure and biological activity [10]. Many eukaryotic proteins similarly fail to fold properly in bacterial expression systems [11] .

## SDS-PAGE and Western Blot Analysis

SDS-PAGE analysis of purified hEGF-linker-$C_H1$ prior to cleavage of the GST affinity tag demonstrated a single band corresponding to a protein with the expected $M_r$ of 44 kDa (Fig. 1 A, lane 1). This band was positive for hEGF by Western blot (Fig. 1 B, Lane 1). There was no 44 kDa band evident on SDS-PAGE in the absence of IPTG induction. The GST affinity tag was cleaved by incubation of the hEGF-linker-$C_H1$ protein with thrombin (10 units/mg) overnight at room temperature. SDS-PAGE of the thrombin-cleaved fusion proteins showed a major band corresponding to a protein with the expected $M_r$ of 18 kDa for hEGF-linker-$C_H1$ (Fig. 1 A, lane 2). This band was also positive by Western blot using an anti-hEGF antibody (Fig. 1 B). There were two closely migrating bands after cleaving hEGF-linker-$C_H1$ with thrombin which were not positive for hEGF by Western blot ($M_r$ 22 kDa and 24 kDa) likely representing thrombin-generated GST fragments. There was a minor band with $M_r$ of 44 kDa positive for hEGF by Western blot indicating some residual hEGF-linker-$C_H1$-GST fusion protein.

*Insert Fig. 1 here.*

**Figure 1:** A. SDS-PAGE analysis of hEGF-linker-$C_H1$ linked to glutathione S-transferase prior to (Lane 1) and after cleavage (Lane 2) with thrombin. B. Corresponding Western blot using anti-hEGF polyclonal antibody.

## Receptor-Binding Properties of hEGF-$C_H1$ and hEGF-linker-$C_H1$

Flow cytometry of A431 epidermoid carcinoma cells or MDA-MB-468 breast cancer cells incubated with hEGF-$C_H1$ without the linker sequence showed a definite shift to increased fluorescence compared to the PBS controls but the magnitude of the fluorescence increase was less for hEGF-$C_H1$ than for hEGF (Fig. 2). The inclusion of the polypeptide linker sequence between hEGF and $C_H1$ significantly improved the binding of the fusion proteins to MDA-MB-468 and A431 cells.

*Insert Fig. 2 here.*

**Figure 2:** Flow cytometry showing binding of hEGF, hEGF-$C_H1$ and hEGF-linker-$C_H1$ to A. MDA-MB-468 breast cancer cells or B. A431 epidermoid carcinoma cells.

ELISA using soluble EGFR coated on a microtiter plate showed that there was no significant difference in the receptor-binding of hEGF or hEGF-linker-$C_H1$ (Fig. 3). Both hEGF and hEGF-linker-$C_H1$ exhibited comparable binding to EGFR at concentrations of 10, 70 or 200 nM.

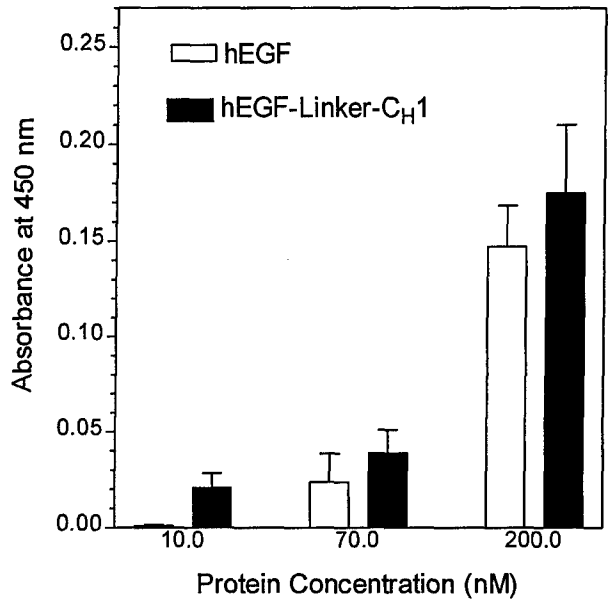


**Figure 3:** ELISA for hEGF and hEGF-linker-$C_H1$ incubated on a microtiter plate coated with soluble EGFR isolated from MDA-MB-468 breast cancer cells. The absorbance is proportional to the amount of hEGF or hEGF-linker-$C_H1$ bound to the wells.

## Tumor and Normal Tissue Biodistribution of hEGF-Linker-$C_H1$ and hEGF Labeled with $^{123}I$

The tumor and normal tissue biodistribution of $^{123}I$-labeled hEGF-linker-$C_H1$ and hEGF are shown in Table 1. Fusion of hEGF with $C_H1$ and the polypeptide linker significantly increased the proportion of radioactivity circulating in the blood at 24 h more than 14-fold (2.72 vs. 0.19 % i.d./g respectively). However, there was no significant difference in tumor uptake between hEGF-linker-$C_H1$ and hEGF (4.25 vs. 4.34 % i.d./g respectively). As a result, the tumor/blood ratios were higher for hEGF than for hEGF-linker-$C_H1$ (23.27 vs. 1.57 respectively). The lower liver and kidney accumulation for $^{123}I$-hEGF-linker-$C_H1$ yielded higher tumor/liver and tumor/kidney ratios than for $^{123}I$-hEGF. The higher stomach and intestinal accumulation for $^{123}I$-hEGF-linker-$C_H1$ compared to $^{123}I$-hEGF suggests an increased deiodination rate *in vivo* for the fusion protein with secretion of free $^{123}I$ into these tissues. The higher stomach and intestinal radioactivity for $^{123}I$-hEGF-linker-$C_H1$ compared to $^{123}I$-hEGF was not due a greater proportion of free $^{123}I$ in the radiopharmaceutical since paper chromatography clearly showed that both radiopharmaceuticals contained <2% free $^{123}I$ at the time of injection. A higher deiodination rate *in vivo* may also have contributed to the lower concentrations of radioactivity in the liver and kidneys for $^{123}I$-hEGF-linker-$C_H1$ compared to $^{123}I$-hEGF. Liver and kidney accumulation of both radiopharmaceuticals are likely mediated by interaction with the moderatetly high levels of EGFR in these tissues [12,13]. Both hEGF and hEGF-linker-$C_H1$ exhibited preserved binding to EGFR on MDA-MB-468 and A431 cells *in vitro* assessed by flow cytometry (Fig. 2) and by ELISA (Fig. 3). Radioiodination of the proteins is not expected to significantly diminish receptor-binding affinity since previous studies in our laboratory [2] demonstrated that hEGF labeled with $^{125}I$ exhibits highly preserved

receptor-binding properties towards MDA-MB-468 cells ($K_a$ 7.3 ± 3.6 × $10^8$; $B_{max}$ 7.2 ± 0.3 × $10^5$ receptors/cell).

**TABLE 1**

Tumor and Normal Tissue Biodistribution for $^{123}$I-hEGF-linker-$C_H1$ and $^{123}$I-hEGF at 24 Hours Post-Injection in Athymic Mice Implanted with s.c. MDA-MB-468 Human Breast Cancer Xenografts

| | *Percent injected dose/g* [a] | | *Tumor/normal tissue ratio* [a] | |
|---|---|---|---|---|
| *Tissue* | *$^{123}$I-hEGF—linker-$C_H1$* | *$^{123}$I-hEGF* | *$^{123}$I-hEGF-linker-$C_H1$* | *$^{123}$I-hEGF* |
| Blood | 2.72 ± 0.09 [b] | 0.19 ± 0.02 [b] | 1.57 ± 0.13 | 23.27 ± 0.78 |
| Heart | 1.84 ± 0.28 | 0.79 ± 0.09 | 2.39 ± 0.27 | 5.72 ± 1.13 |
| Lungs | 2.50 ± 0.23 | 2.79 ± 1.33 | 1.74 ± 0.23 | 3.14 ± 1.89 |
| Liver | 2.48 ± 0.06 | 14.93 ± 0.66 | 1.71 ± 0.09 | 0.29 ± 0.04 |
| Kidneys | 2.70 ± 0.76 | 22.14 ± 1.27 | 2.01 ± 0.80 | 0.20 ± 0.02 |
| Spleen | 0.51 ± 0.11 | 1.68 ± 0.21 | 9.22 ± 2.21 | 2.69 ± 0.48 |
| Stomach | 18.50 ± 1.83 | 2.32 ± 0.44 | 0.23 ± 0.01 | 1.09 ± 0.42 |
| Intestine | 5.18 ± 0.99 | 1.22 ± 0.19 | 0.87 ± 0.16 | 3.67 ± 0.39 |
| Tumor | 4.25 ± 0.25 [c] | 4.34 ± 0.39 [c] | 1.00 | 1.00 |

[a] Mean ± s.e.m. (n =3)
[b] Significantly different (t-test, $p<0.05$)
[c] Not significantly different (t-test, $p>0.05$)

## CONCLUSION

We conclude that fusion of hEGF with the $C_H1$ domain of $IgG_1$ significantly increased its retention in the blood at 24 h after i.v. administration to athymic mice implanted with MDA-MB-468 human breast cancer xenografts but did not significantly increase its tumor uptake. Receptor-binding was relatively preserved *in vitro* for hEGF fused to $C_H1$ particularly with the incorporation of an intervening flexible polypeptide linker but the tumor/blood ratios were decreased for hEGF-linker-$C_H1$ compared to hEGF. These results suggest that the tumor uptake of hEGF is controlled by factors other than its elimination rate from the blood. These factors probably include the high rate of sequestration by normal tissues such as the liver and kidneys which exhibit moderately high levels of EGFR. The high tumor/blood ratios observed for hEGF make the peptide more attractive as a targeting vehicle for EGFR positive tumors for imaging applications than hEGF-linker-$C_H1$.

## ACKNOWLEDGMENTS

This study was supported by grants from the U.S. Army Breast Cancer Research Program (No. DAMD17-98-1-8171) and the Susan G. Komen Breast Cancer Foundation (No. 9749). Parts of this research were presented at the AACR-NCI-EORTC International Conference on Molecular Targets and Cancer Therapeutics, November 16-19, 1999, Washington, DC.

## REFERENCES


1. Klijn JGM, Berns PMJJ, Schmitz PIM, Foekens JA. The clinical significance of epidermal growth factor receptor (EGF-R) in human breast cancer: a review on 5232 patients. *Endocr Rev* 1992; 13: 3.

2. Reilly RM, Kiarash R, Sandhu J, Lee YW, Cameron R, Hendler A, Vallis K, Gariépy J. A comparison of EGF and mAb 528 labeled with indium-111 for imaging human breast cancer. *J Nucl Med* 2000; 41: 903.

3. Hu S, Shively L, Raubitschek A, Sherman M, Williams LE, Wong JYC, Shively JE, Wu AM. Minibody: A novel engineered anti-carcinoembryonic antigen antibody fragment (single-chain Fv-$C_H3$) which exhibits rapid high-level targeting of xenografts. *Cancer Res* 1996; 56: 3055.

4. Skerra A, A general vector, pASK84, for cloning, bacterial production, and single-step purification of antibody Fab fragments. *Gene* 1994; 141: 79.

5. Studier FW, Rosenberg FW, Dunn JJ, Dubendorff JW. Use of T7 RNA polymerase to direct expression of cloned genes. *Methods in Enzymol* 1990; 185: 60.

6. Krupp MN, Connolly DT, Lane MD. Synthesis, turnover, and down-regulation of epidermal growth factor receptors in human A431 epidermoid carcinoma cells and skin fibroblasts. *J Biol Chem* 1982; 257: 11489

7. Filmus J, Trent JM, Pollack MN, Buick RN. Epidermal growth factor receptor gene-amplified MDA-468 breast cancer cell line and its non-amplified variants. *Molec Cellular Biol* 1987; 7: 251.

8. Gregoriou M. *Methods in Molecular Biology*, Vol. 14, Glycoprotein Analysis in Biomedicine Purification of the EGF Receptor for Oligosaccharide Studies. Hounsell EF ed., Humana Press, Totowa, 1993, Chapt. 15: Glycoprotein Analysis in Biomedicine: Purification of the EGF Receptor for Oligosaccharide Studies. pp 189-198.

9. D'Alatri L, Di Massimo AM, Anastasi AM, Pacilli A, Novelli S, Saccinto MP, DeSantis R, Mele A, Parente D. Production and characterization of a recombinant single chain anti ErbB2-clavin immunotoxin. *Anticancer Res* 1998; 18: 3369.

10. Hommel U, Harvey TS, Driscoll PC, Campbell ID. Human epidermal growth factor: High resolution solution structure and comparison with human transforming growth factor α. *J Mol Biol* 1992; 227: 271.

11. Misawa S, Kumagai I. Refolding of therapeutic proteins produced in Escherichia coli as inclusion bodies. *Biopolymers* 1999; 51, 297.

12. Dunn WA, Hubbard AL. Receptor-mediated endocytosis of epidermal growth factor by hepatocytes in the perfused rat liver: ligand and receptor dynamics. *J Cel Biol* 1984; 98: 2148-2159.

13. Fisher DA, Salido EC, Barajas L. Epidermal growth factor and the kidney. *Annu Rev Physiol* 1989; 51: 67-80.

Fig. 1

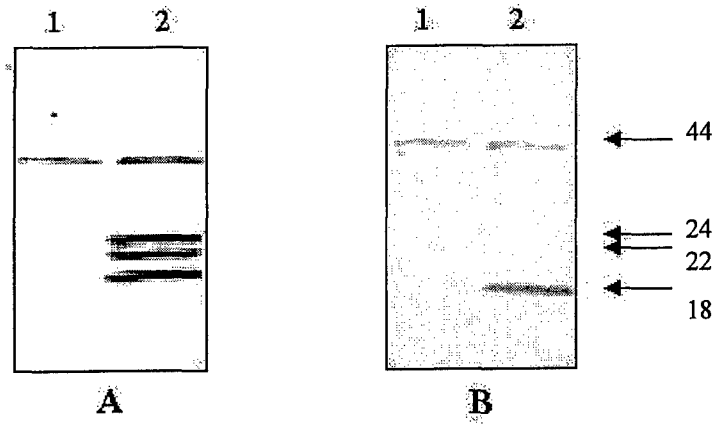

Fig. 2.

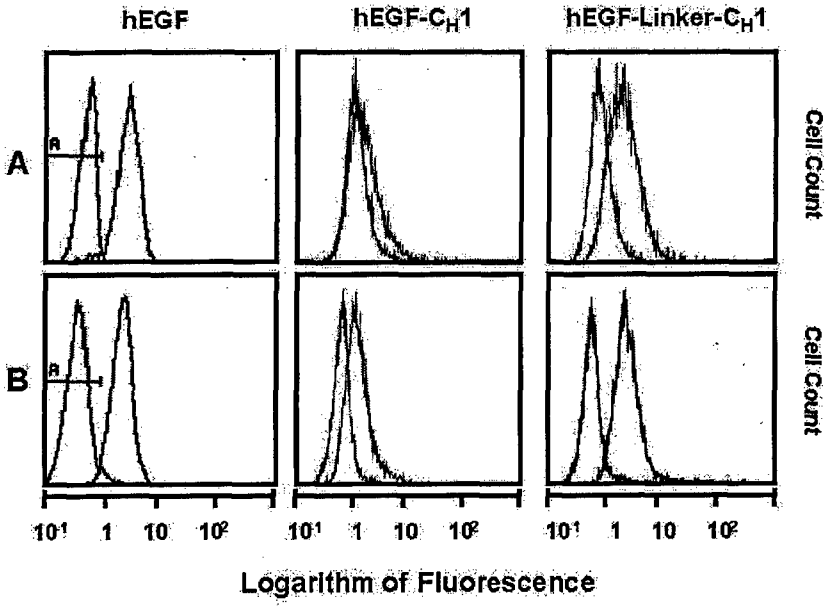
hEGF
hEGF-$C_H1$
hEGF-Linker-$C_H1$
A
B
R
Cell Count
Cell Count
$10^{-1}$ 1 10 $10^2$
$10^{-1}$ 1 10 $10^2$
$10^{-1}$ 1 10 $10^2$
Logarithm of Fluorescence

ELSEVIER

Nuclear Medicine and Biology 28 (2001) 895–902

NUCLEAR MEDICINE — AND — BIOLOGY

# Amplified delivery of indium-111 to EGFR-positive human breast cancer cells

Judy Wang[a], Paul Chen[a], Zi-Fen Su[a], Katherine Vallis[b,e,f], Jasbir Sandhu[d], Ross Cameron[c], Aaron Hendler[a,g], Raymond M. Reilly[a,g,h,*]

[a]*Division of Nuclear Medicine, University Health Network, Toronto General Hospital, Toronto, ON, Canada*
[b]*Department of Radiation Oncology, University Health Network, Princess Margaret Hospital, Toronto, ON, Canada*
[c]*Department of Pathology, University Health Network, Toronto General Hospital, Toronto, ON, Canada*
[d]*Samuel Lunenfeld Research Institute, Mount Sinai Hospital, Toronto, ON, Canada*
[e]*Department of Radiation Oncology, University of Toronto, Toronto, ON, Canada*
[f]*Department of Medical Biophysics, University of Toronto, Toronto, ON, Canada*
[g]*Department of Medical Imaging, University of Toronto, Toronto, ON, Canada*
[h]*Department of Pharmaceutical Sciences, University of Toronto, Toronto, ON, Canada*

Received 15 April 2001; received in revised form 13 July 2001; accepted 21 July 2001

**Abstract**

A method is described to amplify the delivery of $^{111}$In to human breast cancer cells utilizing a novel human serum albumin-human EGF (HSA-hEGF) bioconjugate substituted preferentially in the HSA domain with multiple DTPA metal chelators for $^{111}$In. $^{111}$In-DTPA-HSA-hEGF exhibited a lower receptor-binding affinity than $^{111}$In-DTPA-hEGF but was rapidly and specifically bound, internalized and translocated to the nucleus in EGFR-positive MDA-MB-468 breast cancer cells. $^{111}$In-DTPA-HSA-hEGF was cytotoxic *in vitro* mainly through the emission of short-range Auger electrons and partially through the effects of the hEGF moiety to MDA-MB-468 cells overexpressing EGFR (1–2 × $10^6$ receptors/cell) but not towards MCF-7 breast cancer cells with a 100-fold lower level of EGFR on their surface. The cytotoxicity *in vitro* against MDA-MB-468 cells of $^{111}$In-DTPA-HSA-hEGF substituted with nine DTPA chelators was enhanced 4-fold compared to $^{111}$In-DTPA-hEGF monosubstituted with DTPA. Studies are planned to further evaluate $^{111}$In-DTPA-HSA-hEGF *in vivo* as a new imaging and targeted radiotherapeutic agent for breast cancer. 

*Keywords:* Breast cancer; Indium-111; Epidermal growth factor receptor; Epidermal growth factor; Imaging; Radiotherapy

## 1. Introduction

The epidermal growth factor receptor (EGFR) is an important target for the development of novel agents for treatment of breast cancer [2] since it is overexpressed on the majority of estrogen receptor-negative, hormone-insensitive and poor prognosis forms of the disease [14]. Radiopharmaceuticals directed towards EGFR may allow non-invasive molecular imaging of breast cancer by characterizing tumor receptor status, and thereby predict response to novel therapeutic agents directed towards the receptor. We previously showed that human breast cancer xenografts overexpressing EGFR implanted subcutaneously in athymic mice could be imaged using anti-EGFR monoclonal antibody 528 (mAb 528) or human EGF (hEGF) labeled with $^{111}$In [19]. Tumor accumulation was greatest for $^{111}$In-mAb 528 resulting in higher tumor/blood ratios despite the more rapid blood clearance of $^{111}$In-hEGF. Nevertheless, hEGF has advantages over mAb 528 in that its rapid internalization and nuclear translocation can be exploited to selectively insert $^{111}$In into the cytoplasm and nucleus of EGFR-positive breast cancer cells, where the emitted Auger electrons are highly damaging to DNA, resulting in cell death [18]. Thus, $^{111}$In-hEGF is a promising new radiopharmaceutical for imaging and targeted radiotherapy of EGFR-positive breast cancer.

Receptor-binding proteins are labeled with $^{111}$In by introduction of the strong metal chelator DTPA into the protein, usually by reaction of the bicyclic anhydride of DTPA (cDTPAA) with an ϵ-amino group on a lysine residue or the

* Corresponding author. Tel.: +416-340-3036; fax: +416-340-5065.
*E-mail address:* raymond.reilly@utoronto.ca (R.M. Reilly).

0969-8051/01/$ – see front matter 
PII: S0969-8051(01)00262-1

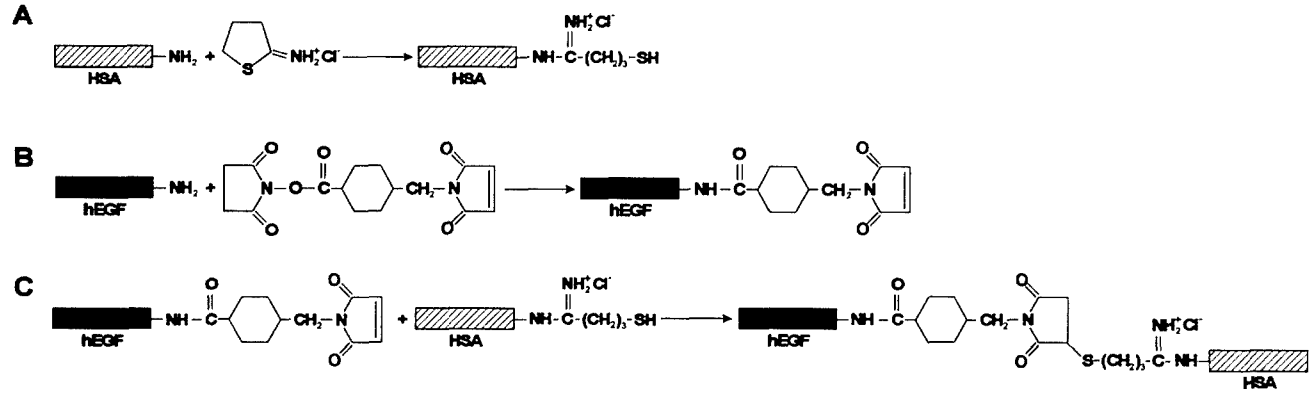


Fig. 1. Construction of HSA-hEGF bioconjugate. A. HSA was thiolated by reaction with 2-iminothiolane. B. hEGF was derivatized with maleimide by reaction with sulfo-SMCC. C. Thiolated HSA was reacted with maleimide-derivatized hEGF.

α-amino group on the protein [11]. In the case of hEGF, there are two lysine residues ($K_{28}$ and $K_{48}$) and the N-terminal asparagine residue which are potential sites for DTPA derivatization. In our experience, reaction of hEGF with a 10-fold molar excess of cDTPAA results in only monosubstitution of the peptide with DTPA, which limits the maximum theoretical specific activity for labeling with $^{111}$In to $<1.8 \times 10^6$ MBq/μmol (approx. 300 MBq/μg). In practice, a specific activity no greater than $2.4 \times 10^5$ MBq/μmol (40 MBq/μg) has been achieved. At this relatively low specific activity, only about 1 in 8 molecules of hEGF carry an $^{111}$In atom and almost 90% of receptors targeted by the radiopharmaceutical are therefore occupied by non-radioactive ligand. This could limit the sensitivity for imaging breast cancer and would restrict the maximum amount of $^{111}$In which can be delivered to breast cancer cells for targeted radiotherapy of the disease.

In this report, we describe a method for amplified delivery of $^{111}$In to EGFR-positive breast cancer cells utilizing a novel human serum albumin-hEGF bioconjugate (HSA-hEGF) multiply substituted with DTPA. The focus of the current communication is the construction and characterization of the $^{111}$In-DTPA-HSA-hEGF bioconjugate with respect to its purity, receptor-binding and internalization as well as its ability to mediate selective cytotoxicity *in vitro* against human breast cancer cells overexpressing EGFR. In future studies, we plan to evaluate $^{111}$In-DTPA-HSA-hEGF *in vivo* in athymic mice implanted subcutaneously with EGFR-positive breast cancer xenografts for imaging and targeted radiotherapy of the disease.

## 2. Materials and methods

### 2.1. Breast cancer cells

MDA-MB-468 and MCF-7 human breast cancer cells displaying approx. $1–2 \times 10^6$ EGFR/cell [5] or $1 \times 10^4$ EGFR/cell respectively were purchased from ATCC (Manassas, VA). MDA-MB-468 cells were cultured in DMEM (Sigma, St. Louis, MO) supplemented with 10% fetal calf serum (FCS) and MCF-7 cells were cultured in α-MEM (Sigma) supplemented with 10% FCS.

### 2.2. Construction and characterization of human serum albumin-hEGF

HSA-hEGF was constructed by reaction of maleimide-derivatized hEGF with thiolated HSA (Fig. 1). Maleimide groups were introduced into hEGF (Upstate Biotechnology, Lake Placid, NY) by reaction of a 4 mg/mL solution of hEGF in phosphate-buffered saline, pH 7.3 (PBS) with a 10-fold molar excess of sulfo-SMCC (Pierce, Rockford, IL) at 37°C for 30 mins. Thiol groups were introduced into HSA (Sigma) by reaction of HSA (10 mg/mL in 150 mM NaCl containing 50 mM triethanolamine and 1 mM disodium EDTA) with a 10-fold molar excess of 2-iminothiolane (Pierce) for 45 mins at room temperature under nitrogen. Meleimide-hEGF was purified on a P-2 mini-column (BioRad, Mississauga, ON) eluted with PBS, then concentrated to 5 mg/mL on a Centricon YM-3 ultrafiltration device (Amicon, Beverly, MA). Thiolated HSA was purified on a Sephadex G-25 mini-column (Pharmacia, Uppsula, Sweden) eluted with PBS containing disodium EDTA, then concentrated to 12 mg/mL on a Centricon YM-30 device. A 3-fold molar excess of maleimide-hEGF was reacted with thiolated HSA overnight at 4°C. Monomeric HSA-hEGF was purified from polymerized species by passage through a Centricon YM-100 device and from excess hEGF by passage through a Centricon YM-30 device.

HSA-hEGF was analyzed for purity and homogeneity by SDS-PAGE, Western blot and size-exclusion HPLC. SDS-PAGE was performed under non-reducing conditions on a 4–20% Tris HCL gradient mini-gel (BioRad) stained with Coomassie R-250 brilliant blue (BioRad). Western blot was conducted by transferring electrophoresed proteins onto a nitrocellulose membrane (Trans-Blot, BioRad) and probing with an anti-HSA (Sigma) or anti-hEGF rabbit polyclonal

antibody (provided by Dr. J. Gariépy, Ontario Cancer Institute). Bands were detected using a goat anti-rabbit antibody conjugated to horseradish peroxidase followed by incubation with diamidobenzidine chromogenic substrate and 0.03% $H_2O_2$. HPLC was performed on a Progel TSK swxl G2000 column eluted with 100 mM $KH_2PO_4$/100 mM $Na_2SO_4$ pH 7.0 at a flow rate of 1 mL/min with UV detection at 280 nm. The hEGF substitution level (moles hEGF/mole HSA) was measured using the ChemiKine Human EGF EIA kit (Chemicon Inc., Ternecula, CA).

### 2.3. Radiolabeling of human serum albumin-hEGF with $^{111}In$

HSA-hEGF was derivatized with multiple DTPA metal chelators by reaction with a 10-fold to 100-fold molar excess of cDTPAA (Sigma) as previously described for hEGF [19]. The conjugation efficiency was measured by trace-labeling an aliquot of the reaction mixture with $^{111}In$ acetate and analyzing the proportion of $^{111}In$-DTPA-HSA-hEGF and free $^{111}In$-DTPA by instant thin layer-silica gel chromatography (ITLC-SG, Gelman, Ann Arbor, MI) developed in 100 mM sodium citrate buffer pH 5.0. DTPA substitution (moles DTPA/mole HSA-hEGF) was calculated by multiplying the conjugation efficiency by the molar ratio of cDTPAA:HSA-hEGF used in the reaction. DTPA-HSA-hEGF was purified on a Sephadex G-50 mini-column eluted with 50 mM $NaHCO_3$ in 150 mM NaCl buffer pH 7.5 then reconcentrated to 10 mg/mL on a Centricon YM-30 device.

DTPA-HSA-hEGF was labeled with $^{111}In$ by incubation with $^{111}In$ acetate for 30 mins at room temperature. $^{111}In$ acetate was prepared by mixing equal volumes of trace-metal free 1 M sodium acetate buffer pH 6.0 and $^{111}In$ chloride (MDS-Nordion, Kanata, ON). For receptor-binding experiments, $^{111}In$-DTPA-HSA-hEGF was labeled to a specific activity of 1–2 MBq/$\mu$g ($5.5 \times 10^4$-$1.1 \times 10^5$ MBq/$\mu$mole). For *in vitro* cytotoxicity studies, $^{111}In$-DTPA-HSA-hEGF was labeled to a higher specific activity of 42 MBq/$\mu$g ($2.7 \times 10^6$ MBq/$\mu$mol) and $^{111}In$-DTPA-hEGF was labeled to 40 MBq/$\mu$g ($2.4 \times 10^5$ MBq/$\mu$mol) as previously described [18]. The radiochemical purity of $^{111}In$-DTPA-HSA-hEGF and $^{111}In$-DTPA-hEGF was >95% by ITLC-SG developed in 100 mM sodium citrate buffer pH 5.0.

### 2.4. Measurement of receptor-binding properties

The receptor-binding properties of $^{111}In$-DTPA-HSA-hEGF were evaluated in a direct radioligand binding assay using MDA-MB-468 human breast cancer cells ($1–2 \times 10^6$ EGFR/cell). Briefly, $^{111}In$-DTPA-HSA-hEGF (40 ng-5 $\mu$g) in 1 mL of 150 mM NaCl containing 0.2% bovine serum albumin was incubated with $3–5 \times 10^6$ cells in 1.5 mL microtubes with occasional mixing for 30 mins at 37°C. Cell bound radioactivity was separated from free radioactivity by centrifugation at 2,700 × g for 5 mins, then counted in a $\gamma$-scintillation counter. Non-specific binding was determined by conducting the assay in the presence of an excess (100 nM) of unlabeled hEGF. Specific binding was obtained by subtraction of non-specific binding from total binding. The $K_a$ and $B_{max}$ values were estimated from a non-linear fitting of the specific binding versus the concentration of $^{111}In$-DTPA-HSA-hEGF using GraphPad Prism software [15].

### 2.5. Determination of internalization and nuclear translocation

Internalization and nuclear translocation was evaluated qualitatively by fluorescence microscopy by incubating a 100 nM solution of fluorescein-conjugated HSA-hEGF in 150 mM NaCl for 1 h at 37°C with $1 \times 10^4$ MDA-MB-468 cells grown overnight on a chamber slide (Nunc, Life Technologies, Burlington, ON). The cells were washed with 150 mM NaCl and counterstained using the nuclear stain DAPI (Boehringer-Mannheim, Laval, PQ), then examined under a fluorescence microscope. In addition, cell fractionation studies were performed with $^{111}In$-DTPA-HSA-hEGF to quantitate the amount of radioactivity internalized by MDA-MB-468 cells and the amount of radioactivity imported into the cell nucleus. Briefly, $1 \times 10^6$ MDA-MB-468 cells in a 35 mm culture dish were incubated with 5 ng of $^{111}In$-DTPA-HSA-hEGF for 30 mins at 37°C. The cells were recovered from the dishes, washed with PBS and centrifuged at 960 × g for 5 mins to separate cell-bound radioactivity from free radioactivity. The proportion of internalized $^{111}In$-DTPA-HSA-hEGF was determined by displacing cell-surface radioactivity with 200 mM sodium acetate/500 mM NaCl pH 2.5 at 4°C. The proportion of radioactivity imported into the cell nucleus was determined by isolating the nuclei by lysing the cells in 10 mM Tris buffer pH 7.6 containing 350 mM sucrose, 10 mM KCl, 1.5 mM $MgCl_2$ and 0.2% Triton X-100 (BioRad) pH 7.6 under ultrasonication for 5 mins and centrifuging the lysate at 2,700 × g. This procedure has previously been found by us [18] and others [16] to result in intact nuclei without contamination by cytoplasmic organelles or fragments of cell membrane.

### 2.6. Determination of cytotoxicity in vitro

The selective cytotoxicity *in vitro* of $^{111}In$-DTPA-HSA-hEGF for human breast cancer cells overexpressing EGFR was evaluated by dispensing $1 \times 10^3$ MDA-MB-468 ($1–2 \times 10^6$ receptors/cell) or MCF-7 cells ($1 \times 10^4$ receptors/cell) into wells in a 96-well culture plate (Nunclon, Canadian Life Technologies, Burlington, ON), culturing the cells overnight, then treating the cells with increasing concentrations (7.5–250 pM) of $^{111}In$-DTPA-HSA-hEGF or $^{111}In$-DTPA-hEGF in growth medium for 7 days. $^{111}In$-DTPA-HSA-hEGF contained nine DTPA groups per molecule and had a specific activity of 42 MBq/$\mu$g ($2.7 \times 10^6$ MBq/$\mu$mol). $^{111}In$-DTPA-hEGF was monosubstituted with

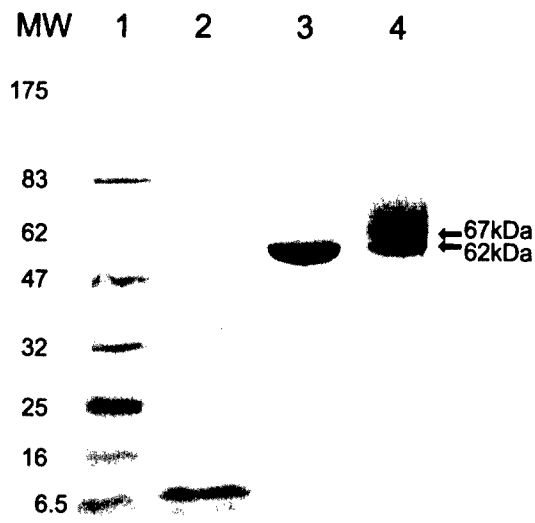


Fig. 2. SDS-PAGE analysis of HSA-hEGF on a non-reducing 4–20% Tris HCl gradient mini-gel stained with Coomassie brilliant blue. Lane 1: Molecular weight standards. Lane 2: hEGF. Lane 3: HSA. Lane 4: HSA-hEGF.

DTPA and had a 10-fold lower specific activity (40 MBq/$\mu$g, 2.4 $\times$ $10^5$ MBq/$\mu$mol). Control wells contained cells cultured in growth medium alone. Cell growth was determined colorimetrically using the WST-1 cell viability assay (Boehringer-Mannheim) by measuring absorbance at 450 nm in a plate reader (Bio-Tek Model ELx800, Winnooski, VT). The concentration of $^{111}$In-DTPA-HSA-hEGF or $^{111}$In-DTPA-hEGF required to cause 50% growth inhibition ($IC_{50}$) was estimated from the growth inhibition curves.

### 2.7. Statistical comparisons

Statistical comparisons were made using Student's t-test ($p < 0.05$).

## 3. Results and discussion

A mostly monomeric HSA-hEGF bioconjugate was produced by reaction of maleimide-HSA with thiolated hEGF as evidenced by the appearance of one major band and a second less intense band on SDS-PAGE, corresponding to proteins with $M_r$ of 62 kDa and 67 kDa respectively (Fig. 2). Only traces of polymerized species of higher molecular weight were observed by SDS-PAGE analysis. SDS-PAGE of unconjugated HSA or hEGF demonstrated one major band corresponding to proteins with the expected $M_r$ of 57 kDa or 6 kDa respectively. Western blot (not shown) confirmed that HSA-hEGF contained both hEGF and HSA moieties. Both the 62 kDa and 67 kDa bands were positive by Western blot for HSA and hEGF moieties, but the most intense band was the 62 kDa band. The Western blot results suggest mostly monosubstitution of HSA with hEGF with a small proportion (<10%) of disubstituted bioconjugate. Size-exclusion HPLC of HSA-hEGF (Fig. 3) showed one major peak with retention time ($t_R$) of 11.8 mins and a second peak with $t_R$ of 10.5 mins. A few additional minor peaks were also observed (including a peak with $t_R$ of 16.0 mins corresponding to unconjugated hEGF), but these accounted for <5% of the total protein concentration. HPLC analysis of unconjugated HSA (not shown) similarly demonstrated two predominant peaks but with slightly longer retention times ($t_R$ of 12.1 mins and 10.8 mins). The small decrease in retention time for the HPLC peaks associated with HSA following hEGF conjugation and the small increase in $M_r$ by SDS-PAGE were in agreement with an hEGF EIA which indicated that the hEGF substitution level was 0.9 $\pm$ 0.1 hEGF molecules/molecule bioconjugate (n = 3).

The receptor-binding affinity for $^{111}$In-DTPA-HSA-hEGF substituted with 1–2 DTPA groups/molecule ($K_a$ 5.1 $\pm$ 1.3 $\times$ $10^7$ L/mole, Table 1) was approximately 15-fold lower than that of similarly substituted $^{111}$In-DTPA-hEGF (7.5 $\pm$ 3.8 $\times$ $10^8$ L/mole) [19]. There was no significant incremental decrease in affinity however as the DTPA substitution level was increased up to 23 DTPA groups/molecule ($K_a$ 3.4 $\pm$ 0.9 $\times$ $10^7$ L/mole). The number of receptors recognized on MDA-MB-468 cells was not significantly different for $^{111}$In-DTPA-HSA-hEGF ($B_{max}$ 1.4–2 $\times$ $10^6$ receptors/cell) or $^{111}$In-DTPA-hEGF ($B_{max}$ 1.3 $\times$ $10^6$ receptors/cell) [19]. These results suggest that the diminished receptor-binding affinity was mainly due to conjugation of hEGF with HSA rather than derivatization with multiple DTPA metal chelators. This would also be consistent with preferential substitution of DTPA onto the HSA moiety, a region of the molecule remote from the receptor-binding domain. HSA contains 60 lysine residues, whereas hEGF contains only two lysines ($K_{28}$ and $K_{48}$) which present $\epsilon$-amino groups for reaction with cDTPAA [9]. Diminished receptor-binding affinity may be due to steric hindrance as a result of reaction of thiolated HSA with hEGF derivatized with maleimide at $K_{48}$, a residue proximal to the putative receptor-binding motif of hEGF [12]. Others have utilized murine EGF (mEGF) which does not contain lysine residues to link macromolecules site-specifically to the $\alpha$-amino group of EGF [8,10]. Although mEGF bioconjugates are reported to exhibit relatively preserved receptor-binding properties, xenogeneic growth factors are known to be immunogenic in humans and may prevent repeated administration for imaging or radiotherapeutic applications [1]. The HSA-hEGF bioconjugate produced was predominantly monosubstituted with hEGF but there may be advantages in a disubstituted hEGF-HSA bioconjugate since this could theoretically increase receptor binding avidity in an analogous manner to that for divalent antibody binding to cell surface antigens. Cross-linking of cell surface EGFR through two hEGF moieties may also promote internalization of the receptor-bioconjugate complex [4].

HSA-hEGF was rapidly internalized and translocated to

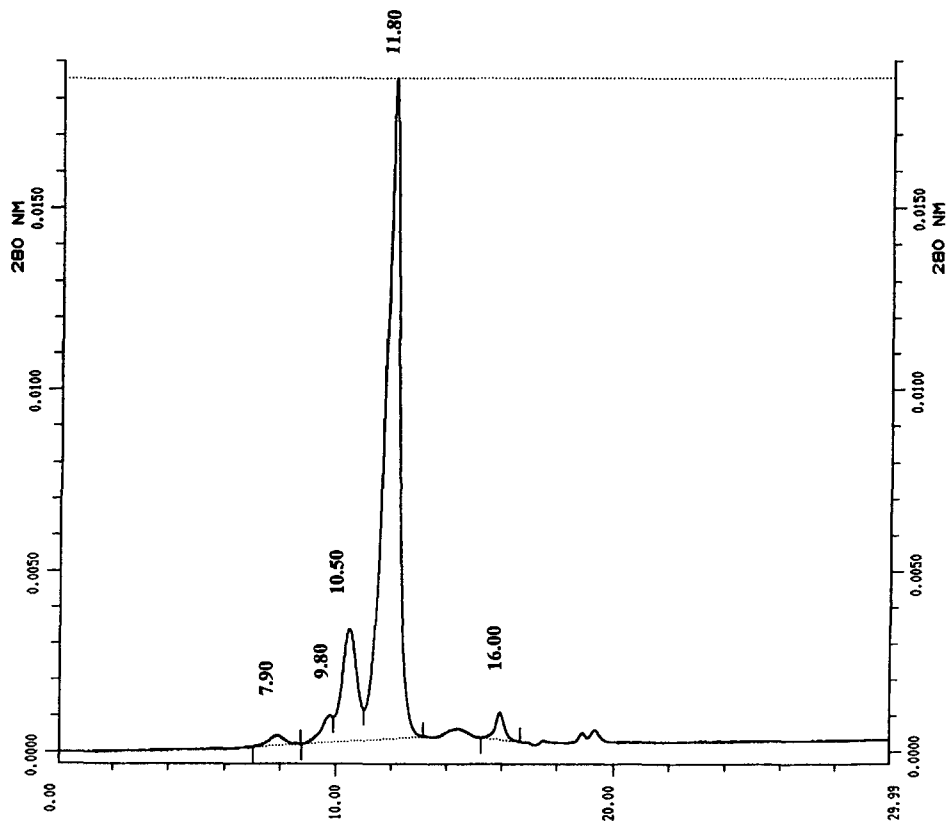


Fig. 3. Size-exclusion HPLC of HSA-hEGF on a Progel TSK swxl G2000 column eluted with 100 mM $KH_2PO_4$/100 mM $Na_2SO_4$ pH 7.0 at a flow rate of 1 mL/min with UV detection at 280 nm.

the nucleus in MDA-MB-468 cells. Fluorescence microscopy of MDA-MB-468 cells incubated with fluorescein-conjugated HSA-hEGF for 30 mins at 37°C (Fig. 4) showed fluorescence on the cell surface, in the cytoplasm and surrounding the cell nucleus (identified by counterstaining with DAPI). Cell fractionation studies with $^{111}$In-DTPA-HSA-hEGF further revealed that 31.1 ± 0.6% of radioactivity remained on the cell surface, 52.6 ± 1.6% was internalized into the cytoplasm and 16.3 ± 2.6% was imported into the cell nucleus within 30 mins at 37°C. The proportion of internalized $^{111}$In-DTPA-HSA-hEGF (approx. 70%) was very similar to that previously measured for $^{111}$In-DTPA-hEGF (approx. 67%) [18], but the fraction of radioactivity imported into the nucleus was about two-fold higher for $^{111}$In-DTPA-HSA-hEGF.

$^{111}$In-DTPA-HSA-hEGF and $^{111}$In-DTPA-hEGF were selectively cytotoxic to MDA-MB-468 cells overexpressing EGFR (Fig. 5A and B). The modest (up to 1.3-fold) growth stimulatory effects of the radiopharmaceuticals on MCF-7 cells may be explained by the mitogenicity of EGF on breast cancer cells with very low EGFR expression [6]. This is in contrast to the effects on breast cancer cells with a high number of EGFR on their surface, which are growth-inhibited by EGF [5]. Since EGF is growth-inhibitory to MDA-MB-468 cells at high concentrations, a small proportion of the cytotoxic effects of $^{111}$In-DTPA-hEGF and $^{111}$In-DTPA-hEGF, particularly at concentrations >50 pM may be due to the hEGF moiety as previously reported [3,18]. $^{111}$In-DTPA-HSA-hEGF was approx. 4-fold more cytotoxic to MDA-MB-468 cells than $^{111}$In-DTPA-hEGF ($IC_{50}$ of 15

Table 1
Receptor-Binding Properties of $^{111}$In-DTPA-HSA-hEGF Multiply Substituted with DTPA

| Molar Ratio (cDTPAA: HSA-hEGF) | DTPA Substitution Level (moles DTPA/mole HSA-hEGF) | $K_a$ (L/mole × $10^7$) | $B_{max}$ (sites/cell × $10^6$) |
|---|---|---|---|
| 10:1 | 1.6 ± 0.6 | 4.1 ± 1.3 | 2.0 ± 0.6 |
| 50:1 | 13.5 ± 2.4 | 4.7 ± 1.3 | 1.6 ± 0.1 |
| 100:1 | 22.7 ± 5.0 | 3.4 ± 0.9 | 1.4 ± 0.1 |

DTPA substitution level and receptor-binding parameters are expressed as mean ± s.e.m. of 3-6 experiments. There were no significant differences (t-test, $p < 0.05$) in $K_a$ or $B_{max}$ values between any of the bioconjugates.

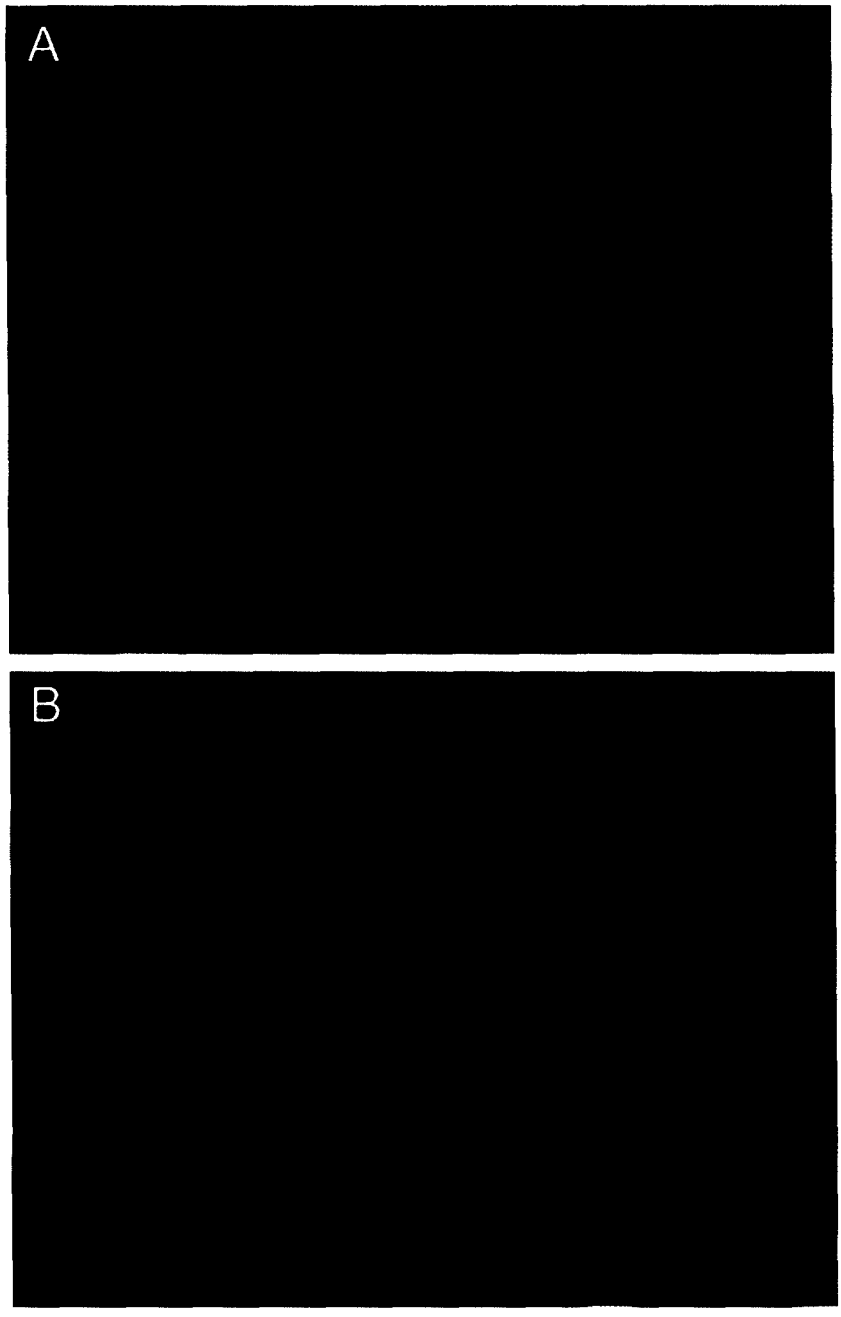


Fig. 4. Fluorescence microscopy of MDA-MB-468 human breast cancer cells incubated with A. fluorescein-derivatized HSA-hEGF or B. DAPI.

pM versus 60 pM respectively). The $IC_{50}$ for unlabeled hEGF on MDA-MB-468 cells is >200 pM (Fig. 5C) [3] indicating that the antiproliferative effects of the radiopharmaceuticals were mediated mainly by the emission of Auger electrons from $^{111}$In. The increase in cytotoxic potency for $^{111}$In-DTPA-HSA-hEGF was lower than expected however, since the specific activity was increased 10-fold compared to $^{111}$In-DTPA-hEGF. This may be due to the reduced receptor-binding affinity of $^{111}$In-DTPA-HSA-hEGF which may decrease the amount of radioactivity targeted to the cells.

One potential limitation to the clinical use of $^{111}$In-DTPA-HSA-hEGF is its 10-fold higher molecular weight compared to $^{111}$In-DTPA-hEGF ($M_r$ 62–67 kDa versus 6 kDa) which could decrease tumor penetration [13,17]. However, monoclonal antibody Fab′ fragments which have a similar molecular size ($M_r$ 50 kDa) penetrate deeply into tumor nodules in human cancer xenograft models [21] and tumor vasculature is known to be "leaky" to macromolecules including plasma proteins such as serum albumin [20]. The lower receptor-binding affinity of $^{111}$In-DTPA-HSA-hEGF compared to $^{111}$In-DTPA-hEGF may facilitate tumor penetration by minimizing the effect of the "binding-site barrier" [7]. It has been theorized that a receptor binding affinity in the range of $5 \times 10^7$-$1 \times 10^8$ L/mole may be optimal to ensure deep tumor penetration and uniformity of intratumoral distribution [7]. Accumulation in normal tis-

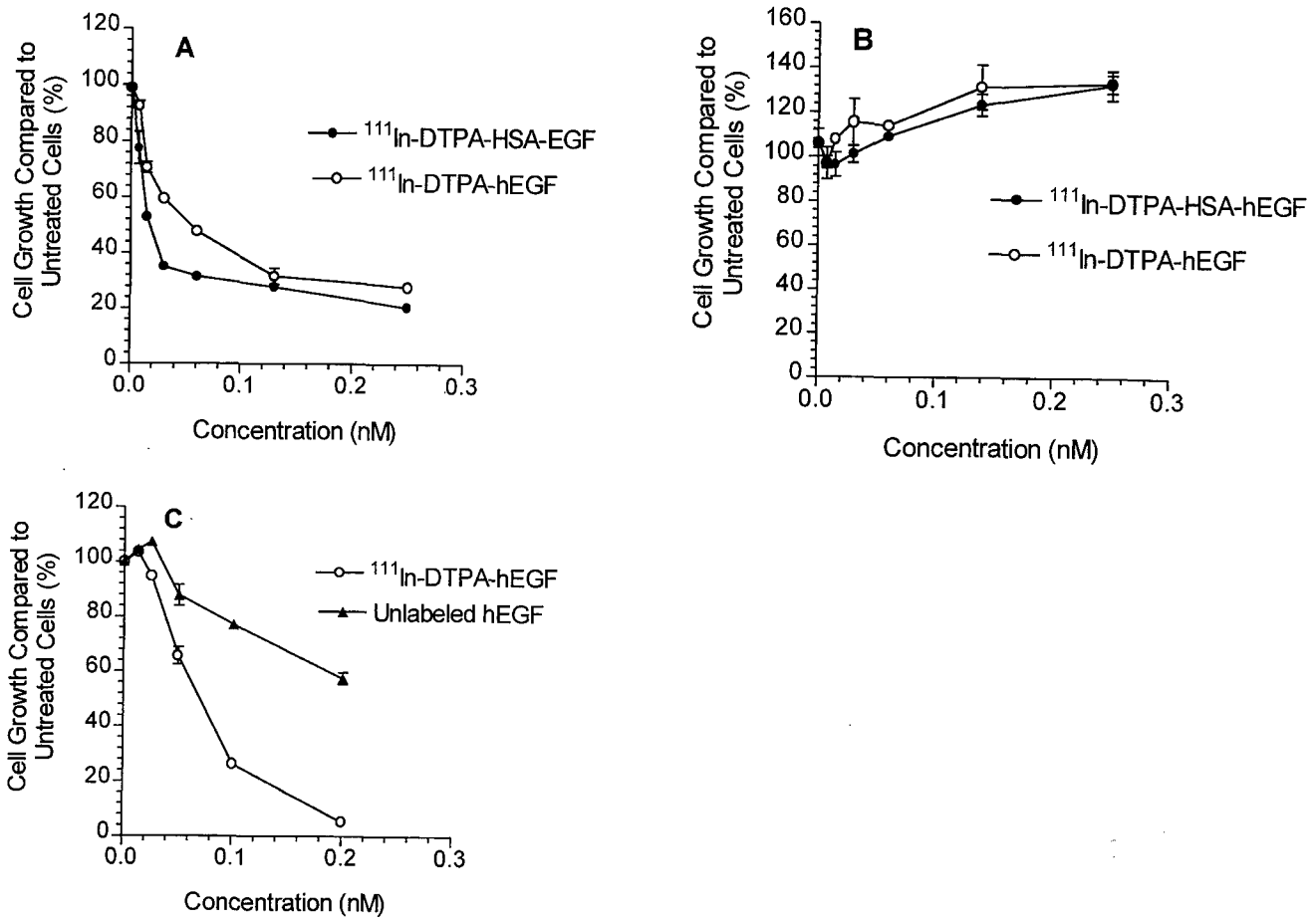


Fig. 5. A. Effect of $^{111}$In-DTPA-HSA-hEGF or $^{111}$In-DTPA-hEGF on the growth of MDA-MB-468 human breast cancer cells overexpressing EGFR (1–2 × $10^6$ receptors/cell) or B. Effect of $^{111}$In-DTPA-HSA-hEGF or $^{111}$In-DTPA-hEGF on the growth of MCF-7 cells with a 100-fold lower level of EGFR expression (1 × $10^4$ receptors/cell). C. Effect of $^{111}$In-DTPA-hEGF or unlabeled hEGF on the growth of MDA-MB-468 human breast cancer cells.

sues which express moderate levels of EGFR such as the liver and kidneys is also an important issue. Our previous experience with $^{111}$In-DTPA-hEGF has shown however that very high amounts of radioactivity (74 MBq/mouse equivalent to a human dose of 14,208 MBq/m$^2$) can be safely administered to mice without any detectable evidence of liver or renal toxicity [18]. This may be due to the quiescent nature of these tissues or to high levels of free-radical scavengers such as glutathione. Future studies are planned to further evaluate the tumor and normal tissue accumulation of $^{111}$In-DTPA-HSA-hEGF *in vivo* in athymic mice implanted subcutaneously with human breast cancer xenografts and the potential utility of the radiopharmaceutical as a novel imaging or radiotherapeutic agent for EGFR-positive breast cancer.

## 4. Conclusions

We have described a method for amplified delivery of $^{111}$In to EGFR-positive human breast cancer cells utilizing a novel HSA-hEGF bioconjugate multiply substituted with DTPA and labeled to high specific activity with $^{111}$In. $^{111}$In-DTPA-HSA-hEGF was specifically bound, internalized and translocated to the nucleus in breast cancer cells. The internalization of the radiopharmaceutical resulted in selective and enhanced cytotoxicity *in vitro* to breast cancer cells overexpressing EGFR mainly through the emission of Auger electrons and partially through the antiproliferative effects of the hEGF moiety. The feasibility of such an amplification strategy has also been successfully demonstrated by others for delivering multiple chlorin-$e_6$ photosensitizers to EGFR-positive breast cancer cells for photodynamic therapy [10] or boron hydride atoms to glioblastomas for boron neutron capture therapy [8]. In this communication, we extend the approach to the delivery of radionuclides to EGFR-positive breast cancer cells.

## Acknowledgments

This study was supported by grants from the U.S. Army Breast Cancer Research Program (No. DAMD17-98-1-

8171) and the Susan G. Komen Breast Cancer Foundation (No. 9749).

## References

[1] L.O. Almer, G. Ekberg, S. Fankhauser, P.D. Home, R. Worth, S. Sailer, A.B. Kurtz, M. Christy, A prospective study of the immunogenicity of porcine insulin in HLA-typed new insulin-treated diabetics, Diabetes Res. 2 (1985) 221–224.

[2] J. Baselga, J. Mendelsohn, The epidermal growth factor receptor as a target for therapy in breast carcinoma, Breast Cancer Res. and Treatment 29 (1994) 127–138.

[3] P. Chen, M. Mrkobrada, K.A. Vallis, R.M. Reilly, Comparative cytotoxicity of Auger electron therapy, γ-radiation and chemotherapeutics against EGFR-positive breast cancer cells, Proc. Am. Assoc. Cancer Res. 41 (2000) 706 (Abstract 4490).

[4] H.S. Earp, T.L. Dawson, X. Li, H. Yu, Heterodimerization and functional interaction between EGF receptor family members: a new signaling paradigm with implications for breast cancer research, Breast Cancer Res Treat 35 (1995) 115–132.

[5] J. Filmus, M.N. Pollak, R. Cailleau, R.N. Buick, A human breast cancer cell line with a high number of epidermal growth factor (EGF) receptors, has an amplified EGF receptor gene and is growth inhibited by EGF, Biochem Biophys Res Commun 128 (1985) 898–905.

[6] S.L. Fitzpatrick, M.P. LaChance, G.S. Schultz, Characterization of epidermal growth factor receptor and action on human breast cancer cells in culture, Cancer Res. 44 (1984) 3442–3447.

[7] K. Fujimori, D.G. Covell, J.E. Fletcher, J.N. Weinstein, A modeling analysis of monoclonal antibody percolation through tumors: a binding site barrier, J. Nucl. Med. 31 (1990) 1191–1198.

[8] L. Gedda, P. Olsson, J. Ponten, J. Carlsson, J, Development and in vitro studies of epidermal growth factor-dextran conjugated for boron neutron capture therapy, Bioconjugate Chem. 7 (1996) 584–591.

[9] Genbank. www.ncbi.nlm.nih.gov Human Serum Albumin. (Accession No. V00495). Bethesda, MD, National Center for Biotechnology Information, 3-1-2000.

[10] A. Gijsens, L. Missiaen, W. Merlevede, P. de Witte, Epidermal growth factor-mediated targeting of chlorin $e_6$ selectively potentiates its photodynamic activity, Cancer Res. 60 (2000) 2197–2202.

[11] D.J. Hnatowich, R.L. Childs, D. Lanteigne, A. Najafi, The preparation of DTPA-coupled antibodies radiolabeled with metallic radionuclides: an improved method, J. Immunol. Meth. 65 (1983) 147–157.

[12] U. Hommel, T.S. Harvey, P.C. Driscoll, I.D. Campbell, Human epidermal growth factor: high resolution solution structure and comparison with human transforming growth factor α, J. Mol. Biol. 227 (1992) 271–282.

[13] R.K. Jain, Physiological barriers to delivery of monoclonal antibodies and other macromolecules in tumors, Cancer Res. 50 (1990) 814s–819s.

[14] J.G.M. Klijn, P.M.J. Berns, P.I.M. Schmitz, J.A. Foekens, The clinical significance of epidermal growth factor receptor (EGF-R) in human breast cancer: a review on 5232 patients, Endocr. Rev. 13 (1992) 3–17.

[15] H.J. Motulsky, P. Stannard, R. Neubig, Prism, Ver 2.0, GraphPad Software Inc, San Diego, 1995.

[16] E.M. Rakowicz-Szulczynska, U. Rodeck, M. Herlyn, H. Koprowski, Chromatin binding of epidermal growth factor, nerve growth factor, and platelet-derived growth factor in cells bearing the appropriate surface receptors, Proc. Natl. Acad. Sci. 83 (1986) 3728–3732.

[17] R.M. Reilly, J. Sandhu, T. Alvarez-Diez, S. Gallinger, J. Kirsh, H.S. Stern, Problems of delivery of monoclonal antibodies: pharmaceutical and pharmacokinetic solutions, Clin. Pharmacokinet. 28 (1995) 126–142.

[18] R.M. Reilly, R. Kiarash, R. Cameron, N. Porlier, J. Sandhu, R.P. Hill, K. Vallis, A. Hendler, J. Gariépy, $^{111}$In-labeled EGF is selectively radiotoxic to human breast cancer cells overexpressing EGFR, J. Nucl. Med. 41 (2000) 429–438.

[19] R.M. Reilly, R. Kiarash, J. Sandhu, Y.W. Lee, R. Cameron, A. Hendler, K. Vallis, J. Gariépy, A comparison of EGF and mAb 528 labeled with $^{111}$In for imaging human breast cancer, J. Nucl. Med. 41 (2000) 903–911.

[20] G. Stehle, H. Sinn, A. Wunder, H.H. Schrenk, J.C.M. Stewart, G. Hartung, W. Maier-Borst, D.L. Heene, Plasma protein (albumin) catabolism by the tumor itself-implications for tumor metabolism and the genesis of cachexia, Crit. Rev. Oncol. Hematol. 26 (1997) 77–100.

[21] T. Yokota, D.E. Milenic, M. Whitlow, J. Schlom, Rapid tumor penetration of a single-chain Fv and comparison with other immunoglobulin forms, Cancer Res. 52 (1992) 3402–3408.

# COMPARATIVE ANTIPROLIFERATIVE EFFECTS OF $^{111}$In-DTPA-hEGF, CHEMOTHERAPEUTIC AGENTS AND γ-RADIATION ON EGFR-POSITIVE BREAST CANCER CELLS

Paul Chen [a], Marko Mrkobrada [f], Katherine A. Vallis [b,e,f], Ross Cameron [c], Jasbir Sandhu [d], Aaron Hendler [a,g] and Raymond M. Reilly [a,g,h]

[a] Division of Nuclear Medicine and Departments of [b] Radiation Oncology and [c] Pathology, University Health Network; [d] Samuel Lunenfeld Research Institute, Mount Sinai Hospital; and Departments of [e] Radiation Oncology, [f] Medical Biophysics, [g] Medical Imaging and [h] Pharmaceutical Sciences, University of Toronto

Abbreviated Title: Antiproliferative effects of $^{111}$In-DTPA-hEGF

Key Words: indium-111; epidermal growth factor; epidermal growth factor receptor; breast cancer; chemotherapy; γ-radiation

Originally submitted: December 7, 2001
Revised: February 28, 2002

Proofed: May 21, 2002

Address correspondence to:
Raymond M. Reilly, PhD
Division of Nuclear Medicine
Toronto General Hospital
University Health Network
Toronto, ON, Canada
M5G 2C4

Tel. (416) 340-3036
FAX: (416) 340-5065
e-mail: raymond.reilly@utoronto.ca

**Abstract**

The antiproliferative effects of $^{111}$In-DTPA-hEGF on breast cancer cells expressing high levels of EGFR were compared with those of chemotherapeutic agents or γ-radiation. MDA-MB-468 cells were cultured with $^{111}$In-DTPA-hEGF (30 MBq/μg, $1.8 \times 10^5$ MBq/μmol), DTPA-hEGF, methotrexate, doxorubicin, paclitaxel or 5-fluorouracil. Cell growth was measured colorimetrically. The $IC_{50}$ for $^{111}$In-DTPA-hEGF was <70 pM (11 kBq/mL) versus 500 pM for DTPA-hEGF. The $IC_{50}$ for paclitaxel, methotrexate, doxorubicin and 5-fluorouracil was 6 nM, 15 nM, 20 nM and 4 μM respectively. $^{111}$In-DTPA-hEGF (70 pM, 11 kBq/mL) delivered approx. 6 Gy to breast cancer cells producing growth inhibition equivalent to 4 Gy of γ-radiation. We conclude that $^{111}$In-DTPA-hEGF exhibited potent antiproliferative effects towards breast cancer cells at concentrations much lower than chemotherapeutic agents and equivalent to those produced by several Gy of high dose rate γ-radiation.

## 1. Introduction

Early detection of breast cancer has improved the prognosis for patients with primary disease confined to the breast but the prognosis for patients with advanced, metastatic breast cancer remains poor. New anticancer treatments which exploit novel mechanisms of cytotoxicity are needed to make an impact on the survival and quality of life of these patients. Targeted radiotherapy using Auger electron-emitting radiopharmaceuticals is one promising novel therapeutic strategy currently being explored for treatment of malignancies [15-17]. Auger electrons are highly damaging to DNA when the radiopharmaceuticals are internalized into the cytoplasm and particularly when imported into the nucleus of cancer cells. Furthermore, the subcellular range of the electrons could minimize or potentially eliminate non-specific normal tissue radiotoxicity (ie. against bone-marrow stem cells) previously found to be dose-limiting for radiopharmaceuticals labeled with longer range, more energetic β-emitters (eg. $^{131}$I or $^{90}$Y-labeled monoclonal antibodies) [20].

Epidermal growth factor (EGF) is a 6 kDa specific peptide ligand for the epidermal growth factor receptor (EGFR), a 170 kDa transmembrane receptor tyrosine kinase overexpressed on 30-50% of human breast cancers (reviewed in [14]). EGFR overexpression in breast cancer is associated with a poor long-term survival, shortened time to recurrence and a low response rate to hormonal therapy [14]. We previously reported that human EGF (hEGF) conjugated to the Auger electron-emitting radionuclide, $^{111}$In was rapidly bound, internalized and translocated to the nucleus in EGFR-positive breast cancer cells [22]. The radiopharmaceutical was highly cytotoxic to MDA-MB-468 human breast cancer cells overexpressing EGFR ($1\text{-}2 \times 10^6$ receptors/cell) reducing their clonogenic survival to <5% at only 111-148 mBq/cell (3-4 pCi/cell), but was not cytotoxic to MCF-7 breast cancer cells exhibiting a 100-fold lower level of EGFR expression. Importantly, $^{111}$In-hEGF was not damaging to normal tissues such as the liver and kidneys which express moderate levels of EGFR ($10^4$-$10^5$ receptors/cell) when high amounts of the radiopharmaceutical (74 MBq equivalent to human doses up to 14.2 GBq) were

administered to mice [22]. Our objective in this study was to directly compare the antiproliferative effects *in vitro* of targeted Auger electron radiotherapy using $^{111}$In-DTPA-hEGF on MDA-MB-468 cells with those produced by selected chemotherapeutic agents or γ-radiation commonly used to treat breast cancer.

## 2. Materials and methods

### *2.1 Breast cancer cells*

MDA-MB-468 human breast cancer cells were obtained from the American Type Culture Collection (ATCC, Manassas, VA) and were cultured in L-15 medium (Sigma, St. Louis, MO) containing 100 units/mL of penicillin, 100 μg/mL of streptomycin, 2 mM L-glutamine and supplemented with 10% fetal calf serum (FCS). MDA-MB-468 cells express 1-2 × $10^6$ EGFR/cell [8].

### *2.2 Radiopharmaceutical*

Human EGF (hEGF, Upstate Biotechnology, Lake Placid, NY) was derivatized with diethylenetriaminepentaacetic acid (DTPA) and labeled to high specific activity (30 MBq/μg, 1.8 × $10^5$ MBq/μmol) with $^{111}$In acetate as previously described [22]. The radiochemical purity of $^{111}$In-DTPA-hEGF was 95-98% measured by instant thin layer chromatography (ITLC-SG) in 100 mM sodium citrate pH 5.0. $^{111}$In-DTPA-hEGF exhibited preserved receptor-binding properties against MDA-MB-468 cells in a direct radioligand binding assay ($K_a$ 7.5 × $10^8$ L/mol; $B_{max}$ 1.3 × $10^6$ EGFR/cell) [21]. $^{111}$In-DTPA-hEGF was sterilized by filtration through a Millex GV 0.22 μm filter (Millipore, Bedford, MA).

### *2.3 Chemotherapeutic agents*

Doxorubicin and methotrexate (Sigma) were dissolved at an initial concentration of 1 mM in sterile 150 mM sodium chloride (Astra). A stock solution of paclitaxel (Sigma, 1 mM) was prepared in tissue culture grade dimethylsulfoxide (DMSO). 5-fluorouracil (5-FU, Sigma) was dissolved at an initial concentration of 300 mM in sterile 150 mM sodium chloride. The stock solutions were stored at 4 °C. Immediately prior to use, the solutions were diluted with serum-free medium to the final concentration to be evaluated and sterilized by filtration through a Millex GV 0.22 μm filter (Millipore, Bedford, MA). The final concentration of DMSO in paclitaxel solutions was <0.01%.

*2.4 Treatment with $^{111}$In-DTPA-hEGF or DTPA-hEGF*

Subconfluent MDA-MB-468 cells were harvested from tissue culture flasks by trypsinization and seeded in triplicate into wells ($10^3$ cells/well) in a 96-well culture plate (Nunclon, Canadian Life Technologies, Burlington, ON). Growth medium was added to each well (100 µL/well) and the cells cultured for 24 hours. The cells were then incubated with $^{111}$In-DTPA-hEGF (4-200 pM, 0.74-37 kBq/mL), DTPA-hEGF (4 pM-2 nM) or phosphate buffered saline pH 7.4 (PBS, negative control) diluted with growth medium and cultured for an additional 7 days.

*2.5 Treatment with chemotherapeutic agents*

MDA-MB-468 cells were seeded in triplicate into wells ($10^3$ cells/well) in a 96-well culture plate and treated for 7 days with paclitaxel (1-25 nM), doxorubicin (3-200 nM), 5-FU (1-20 µM) or methotrexate (2-120 nM) in PBS pH 7.4 (containing 0.01% DMSO for paclitaxel) diluted with growth medium. Negative control wells contained cells incubated with PBS pH 7.4 diluted with growth medium. The growth inhibitory properties of $^{111}$In-DTPA-hEGF (20-200 pM, 3.7-37 kBq/mL) or DTPA-hEGF (10-80 pM) in combination with paclitaxel (5-20 nM) or doxorubicin (25-100 nM) were studied by supplementing the medium with the chemotherapeutic agent after 5 days of incubation with $^{111}$In-DTPA-hEGF and culturing the cells for an additional 2 days. Control wells for combination experiments contained cells treated with $^{111}$In-DTPA-hEGF alone or with DTPA-hEGF alone for 7 days or with paclitaxel or doxorubicin alone for 2 days.

*2.6 Treatment with γ-radiation*

MDA-MB-468 cells were seeded in triplicate into wells ($10^3$ cells/well) in a 96-well culture plate and cultured for 24 hours. The cells were then treated with γ-radiation (2-20 Gy) delivered at 1.1 Gy/min using a $^{137}$Cs source (GC-40E cell irradiator, MDS-Nordion Inc., Kanata, ON) and subsequently cultured for a period of 7 days. Negative control wells contained non-irradiated cells cultured in growth medium.

*2.7 Evaluation of antiproliferative effects*

Growth inhibition of MDA-MB-468 cells was evaluated using a colorimetric cell viability assay (WST-1, Boehringer-Mannheim, Laval, PQ). The cells were treated as described, then the number of viable cells was quantitated by adding WST-1 reagent (10 µL) directly into the wells and incubating the plates for 2 hours at 37 °C. The absorbance of the colored formazan complex formed was measured at 450 nm in a plate reader (Bio-Tek Model ELx800, Winooski, VT). The absorbance of wells containing treated cells was compared to that for control wells containing untreated cells to determine the proportion of cell growth inhibition. The concentration of $^{111}$In-

DTPA-hEGF, DTPA-hEGF or chemotherapeutic agents required to achieve 50% ($IC_{50}$) or 90% ($IC_{90}$) growth inhibition was estimated from the growth inhibition curves. Similarly the amount of γ-radiation (Gy) resulting in a 2-fold ($ED_{50}$) or 10-fold ($ED_{90}$) decrease in the growth of the cells was estimated.

## 3. Results

### *3.1 Treatment with $^{111}$In-DTPA-hEGF or DTPA-hEGF*

At the specific activity achieved in this study (30 MBq/μg, $1.8 \times 10^5$ MBq/μmol), $^{111}$In-DTPA-hEGF strongly inhibited the growth of MDA-MB-468 breast cancer cells *in vitro* with an $IC_{50}$ of 70 pM (11 kBq/mL) and an $IC_{90}$ of 200 pM (37 kBq/mL) (Table 1 and Fig. 1). DTPA-hEGF was also growth inhibitory to MDA-MB-468 cells ($IC_{50}$ of 500 pM and $IC_{90}$ 2 nM) but 7-10 fold less potent than $^{111}$In-DTPA-hEGF. At very low concentrations (<50 pM) there was a slight growth stimulatory effect of DTPA-hEGF on MDA-MB-468 cells. No growth stimulation of MDA-MB-468 cells was observed for $^{111}$In-DTPA-hEGF at any concentration tested (4-200 pM).

### *3.2 Treatment with chemotherapeutic agents*

Paclitaxel was the most potent chemotherapeutic agent exhibiting an $IC_{50}$ of 6 nM and an $IC_{90}$ of 20 nM (Table 1 and Fig. 2). Methotrexate was also effective at inhibiting the growth of MDA-MB-468 cells with an $IC_{50}$ of 15 nM and an $IC_{90}$ of 70 nM. The $IC_{50}$ value for doxorubicin was 20 nM and the $IC_{90}$ value was 75 nM. 5-FU was the least potent chemotherapeutic agent with an $IC_{50}$ of 4 μM and $IC_{90}$ >10 μM (Table 1). The chemotherapeutic agents tested were considerably less effective than $^{111}$In-DTPA-hEGF on a molar concentration basis at inhibiting the growth of MDA-MB-468 cells (Fig. 2). At the specific activity achieved in this study for $^{111}$In-DTPA-hEGF (30 MBq/μg, $1.8 \times 10^5$ MBq/μmol), the most active chemotherapeutic agent, paclitaxel, required an 85-fold higher concentration than the radiopharmaceutical to produce equivalent growth inhibition. A 300-fold higher concentration of doxorubicin, or a 200-fold higher concentration of methotrexate was required to cause growth inhibition of MDA-MB-468 cells similar to that produced by 70 pM (11 kBq/mL) of $^{111}$In-DTPA-hEGF.

The antiproliferative effects of doxorubicin and paclitaxel were evaluated in combination with $^{111}$In-DTPA-hEGF or DTPA-hEGF. Additive antiproliferative effects were achieved by culturing MDA-MB-468 cells with $^{111}$In-DTPA-hEGF or DTPA-hEGF for 5 days followed by supplementing the culture medium with the chemotherapeutic agents for an additional 2 days (Figs. 3 and 4). For example, $^{111}$In-DTPA-hEGF (80 pM, 13 kBq/mL) treatment alone reduced the growth of the cells by 40.4 ± 5.7 %, but when combined with 25, 50 or 100 nM doxorubicin, the growth of the cells was decreased by 57.9 ± 0.1 %, 83.9 ± 4.3 % and 92.8 ± 2.2 % respectively (Fig. 3 A). DTPA-hEGF (80 pM) decreased the growth of MDA-MB-468 cells as a

single treatment by 20.4 ± 3.0 %, but combined with 25, 50 or 100 nM doxorubicin, the growth of the cells was inhibited by 29.1 ± 2.1 %, 31.3 ± 3.3 % and 45.3 ± 4.3 % respectively (Fig. 3 B). The effect of combining paclitaxel with $^{111}$In-DTPA-hEGF was less pronounced (Fig. 4). In this experiment, single modality treatment with $^{111}$In-DTPA-hEGF (100 pM, 16 kBq/mL) reduced the growth of MDA-MB-468 cells by 55.4 ± 6.0 %, but when combined with 5, 10 or 20 nM of paclitaxel, the growth of the cells was decreased by 66.4 ± 5.5 %, 65.8 ± 4.5 % and 72.8 ± 2.1 % (Fig. 4 A). Similarly, DTPA-hEGF (80 pM) decreased the growth of MDA-MB-468 cells by 20.5 ± 3.0 %, but combined with 5, 10 or 20 nM paclitaxel, the growth of the cells was inhibited by 34.7 ± 2.7 %, 46.8 ± 3.0 % and 54.0 ± 1.0 % respectively (Fig. 4 B).

### *3.3 Treatment with γ-radiation*

The $ED_{50}$ for growth inhibition caused by γ-irradiation of MDA-MB-468 cells was 4 Gy and the $ED_{90}$ was 6 Gy (Table 1).

## 4. Discussion

Targeted Auger electron radiotherapy represents a new approach to the management of advanced breast cancer. The results of this study demonstrated that the Auger electron-emitting radiopharmaceutical, $^{111}$In-DTPA-hEGF exhibited stronger antiproliferative effects *in vitro* against MDA-MB-468 human breast cancer cells expressing high levels of EGFR than selected chemotherapeutic agents used for the treatment of the disease. At the specific activity achieved for $^{111}$In-DTPA-hEGF (30 MBq/μg, $1.8 \times 10^5$ MBq/μmol), the radiopharmaceutical was 85-300 fold more potent on a molar concentration basis than paclitaxel, doxorubicin or methotrexate at inhibiting the growth of MDA-MB-468 cells and 4 logarithms more effective than 5-FU. The antiproliferative effects produced by 70-200 pM of $^{111}$In-DTPA-hEGF (11-37 kBq/mL) were similar to those produced by several Gy of high dose rate γ-radiation. Doxorubicin (Adriamycin®), 5-FU and methotrexate are standard chemotherapeutic agents used in the management of metastatic breast cancer and as adjuvent therapy for primary breast cancer, usually in combination with cyclophosphamide (eg. CMF, CAF or FAC regimens) [6]. Paclitaxel (Taxol®) is also active against breast cancer [18] and is being studied as second-line therapy, particularly in combination with high dose cyclophosphamide, thiotepa or melphalan and stem cell rescue [12,25] or as adjuvant therapy for high risk patients [10]. We limited our comparisons to single chemotherapeutic agents due to the complexity of testing combination regimens in a simple *in vitro* cell proliferation assay system, particulary those incorporating cyclophosphamide which requires metabolism *in vivo* to its active metabolites, phosphoramide mustard and acrolein [19]. Similarly we did not evaluate fractionated regimens of γ-radiation since our main objective was to compare targeted Auger electron radiotherapy with $^{111}$In-DTPA-hEGF with single dose γ-irradiation of breast cancer cells.

The antiproliferative effects of $^{111}$In-DTPA-hEGF on MDA-MB-468 cells were mediated mainly by the Auger electron emissions of $^{111}$In, but may also be due in part to the cytotoxicity of the cadmium decay product [2], as well as the growth-inhibitory properties of EGF on breast cancer cells expressing high levels of EGFR [7]. The antiproliferative potency of $^{111}$In-DTPA-hEGF is dependent on the specific activity of the radiopharmaceutical. The theoretical maximum specific activity for $^{111}$In-DTPA-hEGF (300 MBq/μg, $1.8 \times 10^6$ MBq/μmol) is 10-fold higher than that achieved in this study, which suggests that further improvements in the antiproliferative potency of the radiopharmaceutical are possible. We recently reported a novel human serum albumin (HSA)-hEGF bioconjugate multiply substituted with DTPA which was labeled with $^{111}$In to a specific activity (42 MBq/μg, $2.7 \times 10^6$ MBq/μmol) which was 10-fold higher than that obtained in this study for $^{111}$In-DTPA-hEGF [24]. The increased specific activity of $^{111}$In-DTPA-HSA-hEGF amplified the amount of radioactivity delivered to MDA-MB-468 cells *in vitro* and significantly enhanced the growth-inhibitory properties. The antiproliferative effects of unlabeled EGF on MDA-MB-468 cells are thought to be due to p53-independent upregulation of the cyclin-dependent kinase inhibitor p21$^{WAF-1/CIP-1}$ followed by p21$^{WAF-1/CIP-1}$-mediated G1-arrest and induction of apoptosis [1,23].

DNA damage caused by Auger electron-emitting radiopharmaceuticals is dependent on the proximity of the radionuclide decay to DNA [11]. $^{111}$In-DTPA-hEGF is rapidly internalized by MDA-MB-468 cells with 15% of internalized radioactivity imported into the cell nucleus and 10% associating with chromatin [22]. At the $IC_{50}$ of 70 pM (11 kBq/mL) for the radiopharmaceutical, approx. 5% of receptors on MDA-MB-468 cells would be occupied by radioligand assuming a $K_a$ of $7.5 \times 10^8$ L/mol [21]. For a single MDA-MB-468 cell displaying $10^6$ receptors/cell, approx. $5 \times 10^4$ molecules of radiopharmaceutical would be bound and 10% of these ($5 \times 10^3$ molecules) would be expected to translocate to the nucleus and bind to chromatin. At the specific activity of $^{111}$In-DTPA-hEGF (30 MBq/μg, $1.8 \times 10^5$ MBq/μmol), 1 in 10 hEGF molecules carry an $^{111}$In atom. Karamychev et al. [13] have estimated that 0.38 DNA breaks occurred for each $^{111}$In decay in a 42-mer target DNA sequence when hybridized to an $^{111}$In-labeled oligodeoxyribonucleotide. Assuming a similar frequency of DNA cleavage for $^{111}$In-DTPA-hEGF associated with chromatin, about 190 DNA strand breaks may occur in a single MDA-MB-468 breast cancer cell from the decay of 500 chromatin-bound $^{111}$In atoms. Although most DNA strand breaks are repaired, any unrepaired breaks or those repaired incorrectly may be lethal.

DNA damage caused by the Auger electrons emitted by $^{111}$In-DTPA-hEGF is dependent on the radiation absorbed dose to the cell nucleus. Assuming a receptor occupancy of 5% at the $IC_{50}$ (70 pM, 11 kBq/mL) for $^{111}$In-DTPA-hEGF (30 MBq/μg, $1.8 \times 10^5$ MBq/μmol), we estimate that $1.5 \times 10^{-2}$ Bq of $^{111}$In would be delivered to a single MDA-MB-468 cell. The cumulative amount of radioactivity bound per cell (Ã) can be calculated by dividing the radioactivity bound by the decay constant for $^{111}$In ($2.83 \times 10^{-6}$ sec$^{-1}$), assuming rapid cellular uptake and no biological elimination of radioactivity from the cells. At the $IC_{50}$ for $^{111}$In-DTPA-hEGF, Ã would be $5.4 \times 10^3$ Bq × sec. The radiation absorbed dose to the cell nucleus ($\overline{D}$) can then be estimated using the cellular dosimetry model of Goddu et al. [9] as $\overline{D} = \tilde{A} \times S$, where S is the radiation absorbed dose (Gy) per unit of cumulated radioactivity (Gy/Bq × sec) in a subcellular compartment (cell

membrane, cytoplasm or nucleus). The cumulative radioactivity present in each compartment was proportioned according to the previously reported subcellular distribution for $^{111}$In-DTPA-hEGF in MDA-MB-468 cells [22]. These cellular radiation dosimetry calculations estimated that approx. 6 Gy would be absorbed by MDA-MB-468 cells at the $IC_{50}$ for $^{111}$In-DTPA-hEGF (Table 2) and approx. 16 Gy at the $IC_{90}$ (200 pM, 37 kBq/mL).

DeNardo et al. [5] and Clarke et al. [4] showed that combining radioimmunotherapy with paclitaxel significantly enhanced the anti-tumor effects *in vivo* against human breast cancer xenografts in athymic mice compared to either treatment alone. Additive antiproliferative effects were achieved by treating MDA-MB-468 cells with $^{111}$In-DTPA-hEGF *in vitro* for 5 days followed by combined treatment with $^{111}$In-DTPA-hEGF and doxorubicin or paclitaxel for 2 days. Further study is required to determine the optimal doses and sequence of treatments *in vivo*, but these preliminary results nevertheless suggest that combining targeted Auger electron radiotherapy using $^{111}$In-DTPA-hEGF with chemotherapy may be useful for treatment of breast cancer.

We conclude that $^{111}$In-DTPA-hEGF is a highly potent novel radiotherapeutic agent that strongly inhibits the growth *in vitro* of breast cancer cells expressing high levels of EGFR at concentrations several logarithms lower than those required in the case of chemotherapeutic agents. The radiopharmaceutical produced antiproliferative effects at concentrations resulting in estimated radiation absorbed doses of 6-16 Gy, which were similar to those produced by 4-6 Gy of γ-radiation. Tumor growth inhibition studies in athymic mice implanted with s.c. MDA-MB-468 human breast cancer xenografts also recently demonstrated that $^{111}$In-DTPA-hEGF has anti-tumor activity *in vivo*, achieving tumor growth arrest in mice treated with five weekly doses of 18.5 MBq (500 μCi) [3]. These preclinical results are promising for further development of the radiopharmaceutical as a potential new treatment for breast cancer in humans expressing high levels of EGFR.

**Acknowledgements**

This study was supported by grants from the U.S. Army Breast Cancer Research Program (No. DAMD17-98-1-8171) and the Susan G. Komen Breast Cancer Foundation (No. 9749).

## References


1. D.K. Armstrong, S.H. Kaufmann, Y.L. Ottaviano, Y. Furuya, J.A. Buckley, J.T. Isaacs, N.E. Davidson. Epidermal growth factor-mediated apoptosis of MDA-MB-468 human breast cancer cells. Cancer Res 54 (1994) 5280-5283.

2. E.P. Balaban, T.R. Simon, E.P. Frenkel. Toxicity of indium-111 on the radiolabeled lymphocyte. J Nucl Med 28 (1987) 229-233.

3. P. Chen, J. Cameron, J. Wang, K. Vallis, J. Sandhu, J., A.L. Hendler, R.M. Reilly. The anti-tumor effect of the Auger electron-emitting radiopharmaceutical, $^{111}$In-hEGF against MDA-MB-468 human breast cancer xenografts is tumor-size dependent. J Nucl Med 45 (2001) 255P.

4. K. Clarke, F-T. Lee, M.W. Brechbiel, F.E. Smyth, L.J. Old, A.M. Scott. Therapeutic efficacy of anti-Lewis$^{y}$ humanized 3S193 radioimmunotherapy in a breast cancer model: Enhanced activity when combined with taxol. Clin Cancer Res 6 (2000) 3621-3628.

5. S.J. DeNardo, D.L. Kukis, L.A. Kroger, R.T. O'Donnell, K.R. Lamborn, L.A. Miers, D.G. DeNardo, C.F. Meares, G.L. Denardo. Synergy of taxol and radioimmunotherapy with yttrium-90-labeled chimeric L6 antibody: efficacy and toxicity in breast cancer xenografts. Proc Natl Acad Sci USA 94 (1997) 4000-4004.

6. S.M. Fields Jones, H.A. Burris III. Breast cancer, in: E.T. Herfindal and D.R. Gourley (Eds.), Textbook of Therapeutics: Drug and Disease Management, Williams & Wilkins, Baltimore, MD, 1996, pp 1533-1547.

7. J. Filmus, M.N. Polak, R. Cailleau, R. and R.N. Buick. A human breast cancer cell line with a high number of epidermal growth factor (EGF) receptors, has an amplified EGF receptor gene and is growth inhibited by EGF. Biochem Biophys Res Commun 128 (1985) 898-905.

8. J. Filmus, J.M. Trent, M.N. Pollak, R.N. Buick. Epidermal growth factor receptor gene-amplified MDA-468 breast cancer cell line and its non-amplified variants. Molec Cellular Biol 7 (1987) 251-257

9. S.M. Goddu, R.W. Howell, R., D.V. Rao. Cellular dosimetry: absorbed dose fractions for monoenergetic electron and alpha particle sources and S-values for radionuclides uniformly distributed in different cell compartments. J Nucl Med 35 (1994) 303-316.

10. A. Goldhirsch, P. Francis, P., M. Castiglione-Gertsch, R.D. Gelber, and A.S. Coates. Taxanes as adjuvant for breast cancer. Lancet 356 (2000) 507-508.

11. K.G. Hofer, C.R. Harris, M.J. Smith. Radiotoxicity of intracellular Ga-67, I-125 and H-3. Nuclear versus cytoplasmic radiation effects in murine L1210 leukemia cells. Int J Radiat Biol Rel Stud Phys Chem Med 28 (1975) 225-241.

12. W.W. Hu, G.D. Long, K.E. Stockerl-Goldstein, L.J. Johnston, N.J. Chao, R.S. Negrin, K.G. Blume. A feasibility study of multiple cycle therapy with melphalan, thiotepa, and paclitaxel followed by mitoxantrone, thiotepa, and paclitaxel with autologous hematopoietic cell support for metastatic breast cancer. Clin Cancer Res 5 (1999) 3411-3418.

13. V.N. Karamychev, I.G. Panyutin, M-K. Kim, N. Le, C.H. Paik, J.A. Carrasquillo, M.W. Reed, R.D. Neumann. DNA cleavage by $^{111}$In-labeled oligodeoxyribonucleotides. J Nucl Med 41 (2000) 1093-1101.

14. J.G.M. Klijn, P.M.J.J. Berns, P.I.M. Schmitz, J.A. Foekens. The clinical significance of epidermal growth factor receptor (EGF-R) in human breast cancer: a review on 5232 patients. Endocr Rev, 13 (1992) 3-17.

15. E.P. Krenning, P.P.M. Kooij, W.H. Bakker, W.A.P. Breeman, P.T.E. Postema, D.J. Kwekkeboob, H.Y. Oei, M. deJong, T.J. Visser, A.E.M. Reijs, S.W.J. Lamberts. Radiotherapy with a radiolabeled somatostatin analogue, [$^{111}$In-DTPA-D-Phe$^{1}$]-octreotide. A case history. Ann NY Acad Sci 733 (1994) 496-506.

16. E.P. Krenning, R. Valkema, P.P.M. Kooij, W.A.P. Breeman, W.H. Bakker, W.W. deHerder, C.H.J. van Eijck, D.J. Kwekkeboom, M. deJong, S. Pauwels. Peptide receptor radionuclide therapy with [indium 111 DTPA D Phe] octreotide. J Nucl Med 38 Suppl. (1997) 47P.

17. G. Mariani, L. Bodei, S.J. Adelstein, A.I. Kassis. Emerging roles for radiometabolic therapy of tumors based on Auger electron emission. J Nucl Med 41 (2000) 1519-1521.

18. D.E. McCloskey, S.H. Kaufmann, L.J. Prestigiacomo, N.E. Davidson. Paclitaxel induces programmed cell death in MDA-MB-468 human breast cancer cells. Clin Cancer Res 2 (1996) 847-854.

19. M.J. Moore and C. Erlichman, C. Pharmacology of anticancer drugs, in: I.F. Tannock and R.P. Hill (Eds.), The Basic Science of Oncology 3$^{rd}$ ed., McGraw Hill, Toronto, 1998. pp 370-391.

20. R.M. Reilly, J.S. Sandhu, T. Alvarez-Diez, S. Gallinger, J. Kirsh, H.S. Stern. Problems of delivery of monoclonal antibodies: Pharmaceutical and pharmacokinetic solutions. Clin Pharmacokinet, 28 (1995) 126-142.

21. R.M. Reilly, R. Kiarash, J. Sandhu, Y.W. Lee, R. Cameron, A. Hendler, K. Vallis, J. Gariépy. A comparison of epidermal growth factor and monoclonal antibody 528 labeled with indium-111 for imaging human breast cancer. J Nucl Med 41 (2000) 903-911

22. R.M. Reilly, R. Kiarash, R., Cameron, N. Porlier, J. Sandhu, R.P. Hill, K. Vallis, A. Hendler, J. Gariépy. Indium-111 labeled EGF is selectively radiotoxic to human breast cancer cells overexpressing EGFR. J Nucl Med, 41 (2000) 429-438.

23. T. Thomas, S. Balabhadrapathruni, C.R. Gardner, J. Hong, C.A. Faaland, and T.J. Thomas. Effects of epidermal growth factor on MDA-MB-468 breast cancer cells: alterations in polyamine biosynthesis and the expression of p21/CIP1/WAF1. J Cellular Physiol 179 (1999) 257-266.

24. J. Wang, P. Chen, Z-F. Su, K. Vallis, J. Sandhu, R. Cameron, A. Hendler, R.M. Reilly. Amplified delivery of indium-111 to EGFR-positive human breast cancer cells. Nucl Med Biol 28 (2001) 895-902.

25. T.M. Zimmerman, D.L. Grinblatt, R. Malloy, S.F. Williams. A phase I dose escalation trial of continuous infusion paclitaxel to augment high dose cyclophosphamide and thiotepa plus stem cell rescue for the treatment of patients with advanced breast carcinoma. Cancer 83 (1998) 1540-154

Table 1.

Inhibition of the Growth of MDA-MB-468 Human Breast Cancer Cells Treated *in vitro* with $^{111}$In-DTPA-hEGF, DTPA-hEGF, Chemotherapeutic Agents or γ-Radiation*.

| Treatment | Range Studied | $IC_{50}$ or $ED_{50}$ | $IC_{90}$ or $ED_{90}$ |
|---|---|---|---|
| $^{111}$In-DTPA-hEGF | 4-200 pM | 70 pM<br>(11 kBq/mL) | 200 pM<br>(37 kBq/mL) |
| DTPA-hEGF | 4 pM-2 nM | 500 pM | 2 nM |
| Paclitaxel | 1-25 nM | 6 nM | 20 nM |
| Methotrexate | 2-120 nM | 15 nM | 70 nM |
| Doxorubicin | 3-200 nM | 20 nM | 75 nM |
| 5-Fluorouracil | 1-20 μM | 4 μM | >10 μM |
| γ-Radiation | 2-20 Gy | 4 Gy | 6 Gy |

* MDA-MB-468 cells were treated *in vitro* with $^{111}$In-DTPA-hEGF (30 MBq/μg, $1.8 \times 10^5$ MBq/μmol), DTPA-hEGF, chemotherapeutic agents or γ-radiation and the growth of the cells compared to untreated cells over 7-days was measured colorimetrically using the WST-1 assay.

Table 2.

Radiation Absorbed Dose Estimates for Treatment of MDA-MB-468 Human Breast Cancer Cells with $^{111}$In-DTPA-hEGF*

| Cell compartment | Ã† (Bq × sec) | S ([Gy/Bq × sec] × $10^{-4}$) | Radiation absorbed dose to cell nucleus, $\overline{D}$ (Gy) |
|---|---|---|---|
| Cell membrane | 1,060 | 1.78 | 0.19 |
| Cytoplasm | 3,440 | 3.18 | 1.09 |
| Nucleus | 790 | 60.30 | 4.76 |
| | | Total: | 6.04 |

* The cellular radiation dosimetry model of Goddu et al. [9] was used to estimate the radiation absorbed dose ($\overline{D}$) to the cell nucleus: $\overline{D} = \tilde{A} \times S$, where S is the radiation absorbed dose (Gy) per unit of cumulated radioactivity (Gy/Bq × sec) in a subcellular compartment.

† Based on treatment of MDA-MB-468 cells *in vitro* with $^{111}$In-DTPA-hEGF (30 MBq/μg, 1.8 × $10^5$ MBq/μmol) at the $IC_{50}$ (70 pM, 11 kBq/mL). The cumulative amount of $^{111}$In-DTPA-hEGF delivered to each cell was 5.3 × $10^3$ Bq × sec, obtained by dividing the amount of radioactivity bound per cell at the $IC_{50}$ (1.5 × $10^{-2}$ Bq) by the decay constant for $^{111}$In (2.83 × $10^{-6}$ $sec^{-1}$) assuming no biological elimination. The reported subcellular distribution of $^{111}$In-DTPA-hEGF [22] was used to calculate the proportion of radioactivity present on the cell membrane, internalized into the cytoplasm or imported into the cell nucleus.

**Legends for Figures**

Fig. 1. Inhibition of the growth of MDA-MB-468 human breast cancer cells *in vitro* by increasing molar and radioactivity concentrations of $^{111}$In-DTPA-hEGF (specific activity 30 MBq/μg, $1.8 \times 10^5$ MBq/μmol) or increasing molar concentrations of DTPA-hEGF.

Fig. 2. Inhibition of the growth of MDA-MB-468 breast cancer cells *in vitro* by increasing molar concentrations of $^{111}$In-DTPA-hEGF (specific activity 30 MBq/μg, $1.8 \times 10^5$ MBq/μmol), paclitaxel, methotrexate or doxorubicin.

Fig. 3. Inhibition of the growth of MDA-MB-468 breast cancer cells *in vitro* by A. increasing molar concentrations of $^{111}$In-DTPA-hEGF (specific activity 30 MBq/μg, $1.8 \times 10^5$ MBq/μmol) alone or combined with doxorubicin (25-100 nM) or B. increasing molar concentrations of DTPA-hEGF alone or combined with doxorubicin (25-100 nM).

Fig. 4. Inhibition of the growth of MDA-MB-468 breast cancer cells *in vitro* by A. increasing molar concentrations of $^{111}$In-DTPA-hEGF (specific activity 30 MBq/μg, $1.8 \times 10^5$ MBq/μmol) alone or combined with paclitaxel (5-20 nM) or B. increasing molar concentrations of DTPA-hEGF alone or combined with paclitaxel (5-20 nM).

Fig. 1.

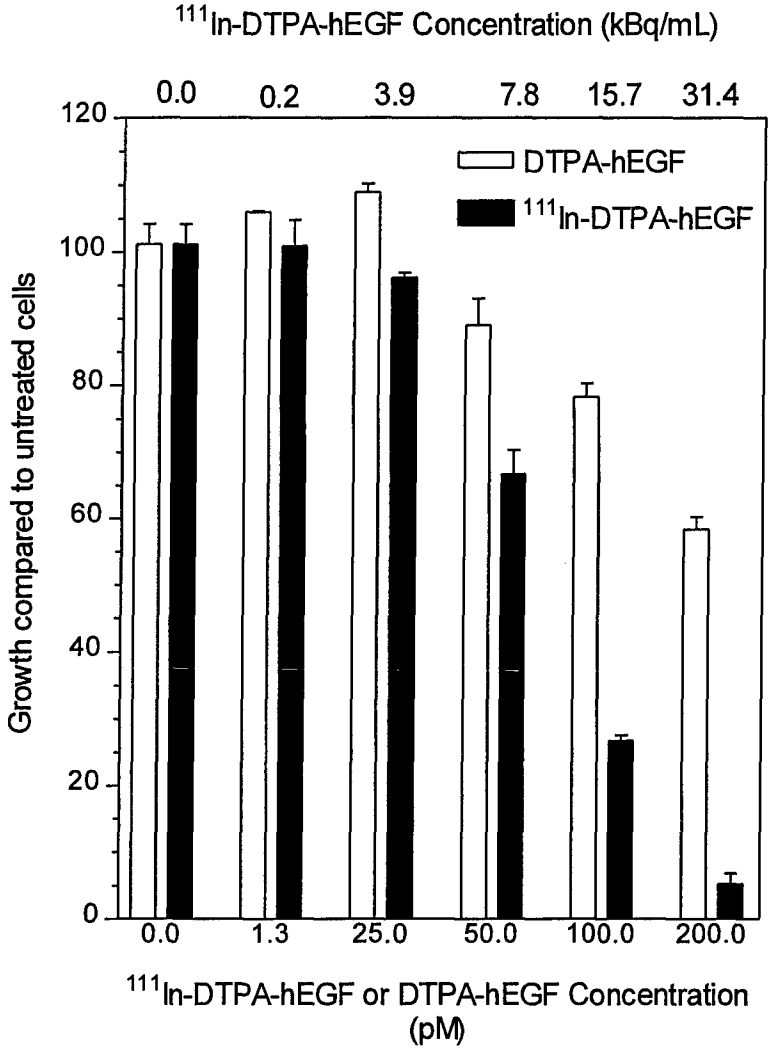
111In-DTPA-hEGF Concentration (kBq/mL)
0.0
0.2
3.9
7.8
15.7
31.4
120
100
80
60
40
20
0
DTPA-hEGF
111In-DTPA-hEGF
Growth compared to untreated cells
0.0
1.3
25.0
50.0
100.0
200.0
111In-DTPA-hEGF or DTPA-hEGF Concentration (pM)

Fig. 2

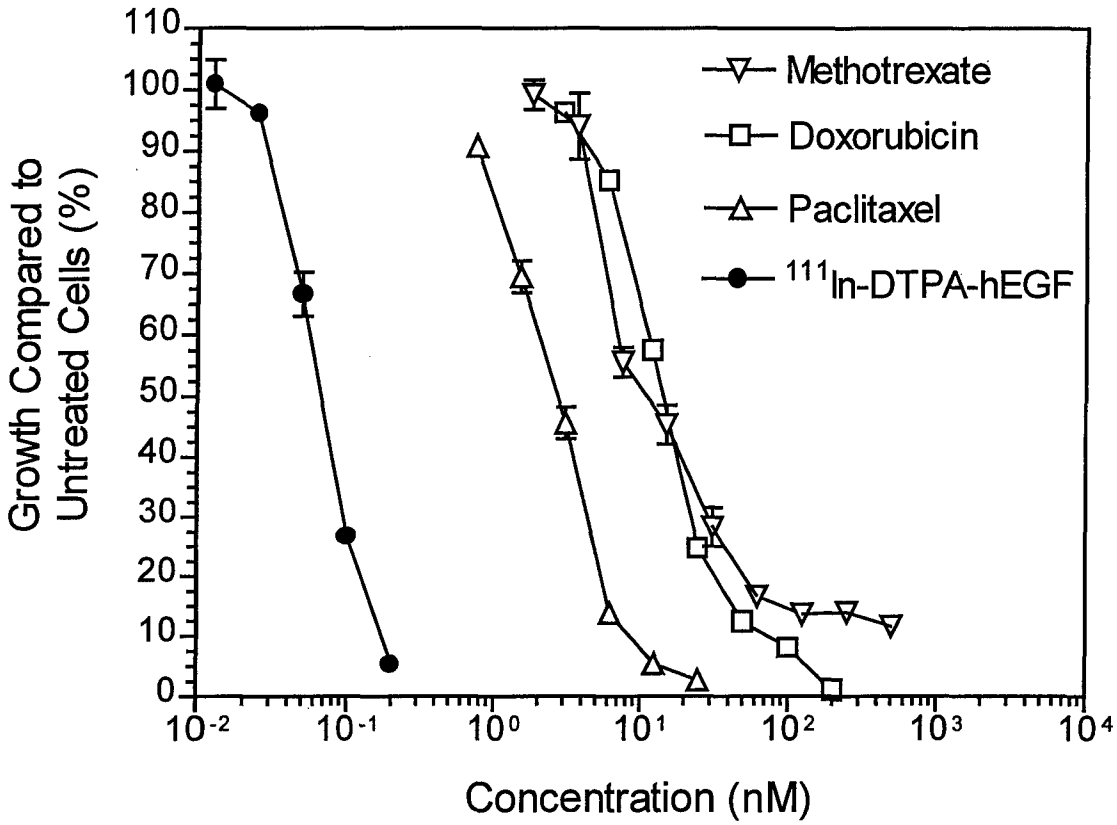
Growth Compared to Untreated Cells (%)
110
100
90
80
70
60
50
40
30
20
10
0
$10^{-2}$
$10^{-1}$
$10^{0}$
$10^{1}$
$10^{2}$
$10^{3}$
$10^{4}$
Concentration (nM)
Methotrexate
Doxorubicin
Paclitaxel
$^{111}$In-DTPA-hEGF

Fig. 3.

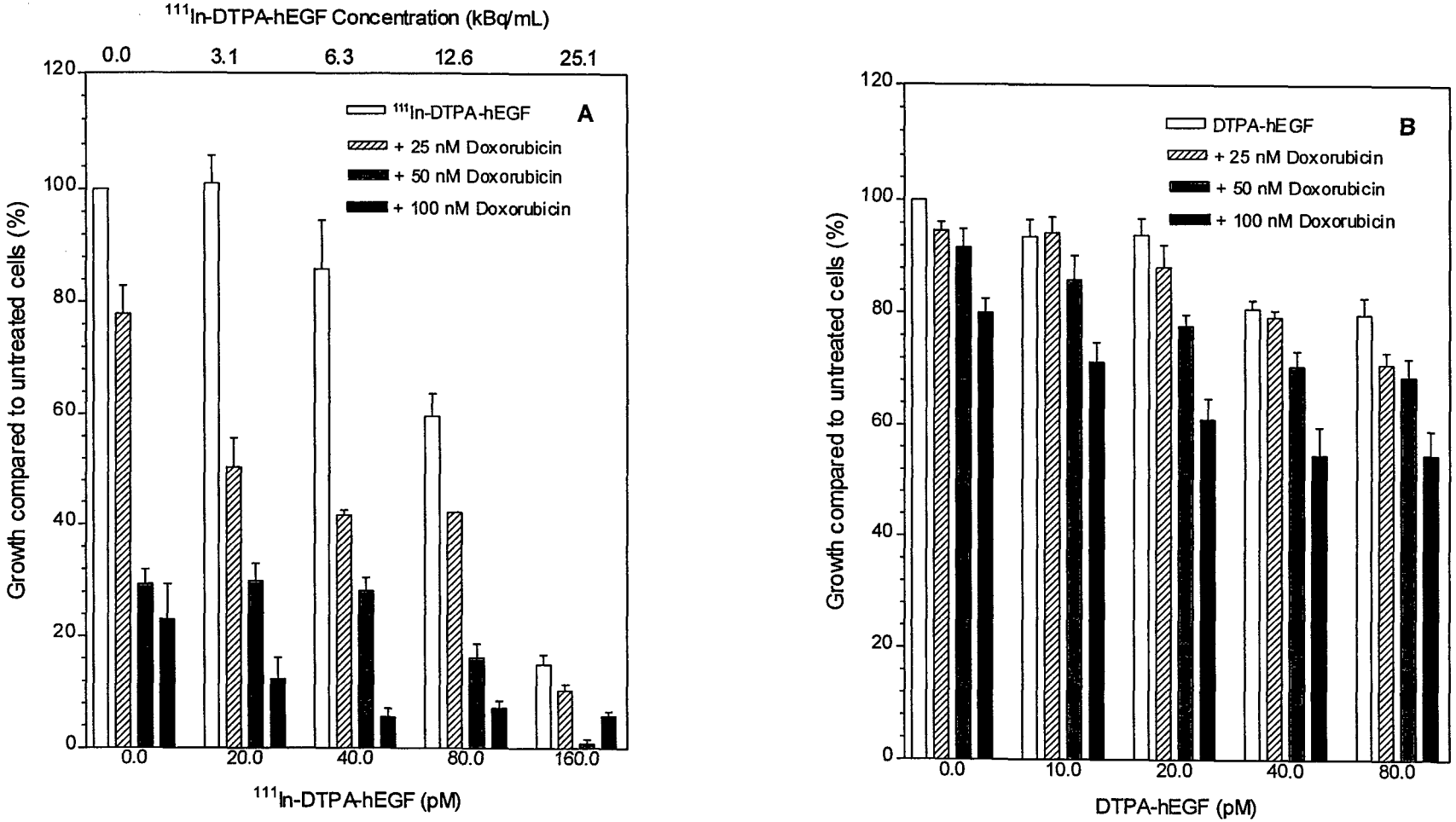
111In-DTPA-hEGF Concentration (kBq/mL)
0.0
3.1
6.3
12.6
25.1
111In-DTPA-hEGF
A
+ 25 nM Doxorubicin
+ 50 nM Doxorubicin
+ 100 nM Doxorubicin
Growth compared to untreated cells (%)
120
100
80
60
40
20
0
0.0
20.0
40.0
80.0
160.0
111In-DTPA-hEGF (pM)
DTPA-hEGF
B
+ 25 nM Doxorubicin
+ 50 nM Doxorubicin
+ 100 nM Doxorubicin
Growth compared to untreated cells (%)
120
100
80
60
40
20
0
0.0
10.0
20.0
40.0
80.0
DTPA-hEGF (pM)

Fig. 4.

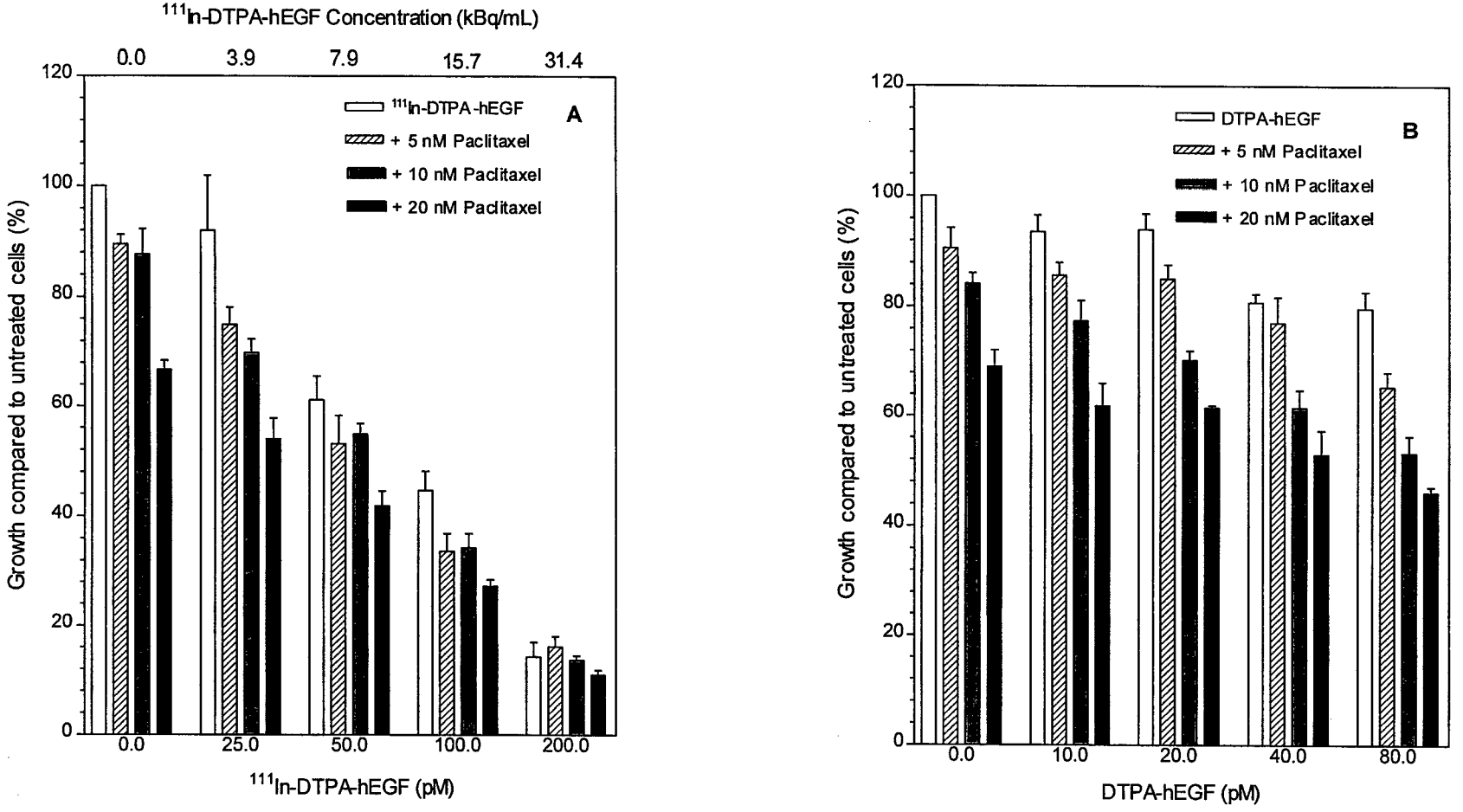
111In-DTPA-hEGF Concentration (kBq/mL)
0.0
3.9
7.9
15.7
31.4
Growth compared to untreated cells (%)
111In-DTPA-hEGF
+ 5 nM Paclitaxel
+ 10 nM Paclitaxel
+ 20 nM Paclitaxel
A
0.0
25.0
50.0
100.0
200.0
111In-DTPA-hEGF (pM)
DTPA-hEGF
+ 5 nM Paclitaxel
+ 10 nM Paclitaxel
+ 20 nM Paclitaxel
B
0.0
10.0
20.0
40.0
80.0
DTPA-hEGF (pM)